Inaugural-Dissertation zur Erlangung der Doktorwürde der Tierärztlichen Fakultät der Ludwig-Maximilians-Universität München

Untersuchung der relativen zellulären Glukoseaufnahme von Mikrogliazellen im regulären Hirnmilieu

vorgelegt von

Sebastian Thomas Kunte

aus

München

München 2026

Aus dem Veterinärwissenschaftlichen
Department der Tierärztlichen Fakultät
der Ludwig-Maximilians-Universität
München

Lehrstuhl für Molekulare Tierzucht und
Biotechnologie

Arbeit angefertigt unter der Leitung von:
Univ.-Prof. Dr. Eckhard Wolf

Angefertigt in der Klinik und Poliklinik
für Nuklearmedizin
Klinikum der Universität München

Mentor: Prof. Dr. Dr. Matthias Brendel

Gedruckt mit der Genehmigung der Tierärztlichen Fakultät
der Ludwig-Maximilians-Universität München

Dekan:	Univ.-Prof. Dr. Reinhard K. Straubinger, Ph.D.
Berichterstatter:	Univ.-Prof. Dr. Eckhard Wolf
Korreferent/en:	Univ.-Prof. Dr. Kaspar Matiasek Univ.-Prof. Dr. Nicolai T. Siegel Prof. Dr. Sabine André Univ.-Prof. Dr. Cornelia A. Deeg

Tag der Promotion: 7. Februar 2026

Meinen Eltern und meiner Schwester

Inhaltsverzeichnis

Abkürzungsverzeichnis

AD	Alzheimer Demenz / Engl. Alzheimer’s disease
ATP	Adenosintriphosphat
CT	Computertomographie / Engl. computed tomography
FACS	Durchflusszytometrie / Engl. fluorenscence activated cell sorting
fMRT	Funktionelle Magnetresonanztomographie
^{18}F-FDG	Engl. ^{18}F-Fluoro-2-deoxy-2-D-glucose
MACS	Immunomagnetisches cell sorting / Engl. magnetic activated cell sorting
MRT	Magnetresonanztomographie
PET	Positronenemissionstomographie / Engl. positron emission tomography
scRadiotracing	Engl. single cell Radiotracing

Die dieser Dissertationsschrift zugrundeliegende Originalarbeit wurde am 15.08.2025 als Publikation mit dem Titel „Distinct reduction in relative microglial glucose uptake compared to astrocytes and neurons upon isolation from the brain environment“ im wissenschaftlichen Fachjournal Frontiers in Cellular Neuroscience zur Veröffentlichung angenommen.

Volume 19 – 2025; https://doi.org/10.3389/fncel.2025.1572431.

1. Beitrag zur Publikation

1.1 Eigenanteil an “Distinct reduction in relative microglial glucose uptake compared to astrocytes and neurons upon isolation from the brain environment”

Ausarbeitung des Konzeptes der vorliegenden Studie zum direkten Vergleich der *in vivo* und *in vitro* ^{18}F-FDG-Traceraufnahme gemeinsam mit dem Betreuer Professor Brendel, basierend auf zuvor generierten Ergebnissen. Mitarbeit bei der Etablierung des zugrundeliegenden neuartigen Ansatzes zur Quantifizierung und Rückverfolgung der zerebralen Radiotraceraufnahme auf zellulärer Ebene mit Laura M. Bartos und dem Betreuer. Erörterung und Evaluierung der Versuchsergebnisse sowie methodischer Fragestellungen. Planung der Panel- und Gating-Strategie für die Durchflusszytometrie sowie Auswertung der Daten. Eigenständige Durchführung, Auswertung und statistische Analyse aller Versuche sowie Erstellung der Abbildungen für die Publikation. Interpretation der Ergebnisse sowie Verfassen des Manuskriptentwurfs unter Supervision des Betreuers.

2. Einleitung

Veränderungen des zellulären mitochondrialen Energiestoffwechsels im Gehirn sowie charakteristische metabolische Muster sind gemeinhin als wichtige Indikatoren neurodegenerativer Erkrankungen, wie Morbus Alzheimer anerkannt. Diese können den klassischen pathologischen Merkmalen, wie der Anwesenheit seniler Plaques und neurofibrillären Bündeln, zeitlich weit vorausgehen [1-6]. Hieraus ergibt sich ein stetig wachsendes Interesse an der Untersuchung von in der Pathogenese involvierten zerebralen Stoffwechselvorgängen und eine Vielzahl von Methoden, um diese *in vivo* und *in vitro* nachzuvollziehen und zu quantifizieren.

Morbus Alzheimer ist gemäß der S3-Leitlinie „Demenzen“ als primär neurodegenerative zerebrale Krankheit klassifiziert und stellt die häufigste Form von Demenz dar. Im Zuge der chronischen bis progressiven Erkrankung manifestieren sich Störungen vieler höherer kortikaler Funktionen, wie beispielsweise Gedächtnis, Orientierung und Urteilsvermögen. Die zugrundeliegenden Pathomechanismen umfassen die Akkumulation extrazellulärer Amyloid-β-Plaques und abnormaler intrazellulärer Tau-Proteine sowie schwerwiegende Veränderungen des zerebralen Metabolismus [7-11]. Insgesamt liegt der Alzheimer Demenz (AD) demnach eine komplexe Pathogenese zugrunde, die der Diagnostik und Therapie verschiedene Ansatzmöglichkeiten bietet.

In der klinischen Routinediagnostik ist die Positronen-Emission-Tomographie (PET) fest etabliert [12-14]. Dabei werden Radioliganden (Tracer) eingesetzt, die an spezifische Zielmoleküle (Targets) binden oder im Falle von ^{18}F-Fluoro-2-deoxy-2-D-glucose (^{18}F-FDG) unspezifisch, in Korrelation mit der metabolischen Aktivität, in Zellen aufgenommen werden. ^{18}F-FDG wird nach Aufnahme in die Zelle durch die Hexokinase Reaktion phosphoryliert. Dies verhindert, dass das Glukosemolekül die Zelle wieder verlassen kann. Anders als physiologisches Glukose-6-phosphat kann das verwendete Deoxyglukose-6-phosphat zudem nicht als Substrat in die Glykolyse einfließen und akkumuliert daher in der Zelle [15, 16]. Die PET in Kombination mit einer Computertomographie (^{18}F-FDG-PET/CT) kann ^{18}F-FDG somit für die Dauer seiner Gammaemissionen, räumlich und zeitlich aufgelöst, exakt lokalisieren. Dieses Bildgebungsverfahren erlaubt die Identifizierung von Zellverbänden mit gesteigerter oder reduzierter Glukoseaufnahme und folglich mit verändertem Metabolismus sowie die Zuordnung einer bestimmten Hirnregion. Infolgedessen lassen sich mit dieser

diagnostischen Methode Alzheimer und nicht-Alzheimer Demenzen unterscheiden [17]. Die Ursache der pathologischen Veränderungen des PET-Signals auf zellulärer Ebene blieb dabei allerdings lange ungeklärt, da ^{18}F-FDG unspezifisch von allen Zellen aufgenommen werden kann [18].

Um dieser Problematik im Rahmen präklinischer Forschung auf den Grund zu gehen, haben wir und andere Arbeitsgruppen einen neuartigen Workflow (single cell Radiotracing, scRadiotracing) etabliert und weiterentwickelt, welcher die Quantifizierung der Traceraufnahme auf zellulärer Ebene ermöglicht. Die ^{18}F-FDG-PET/CT und das scRadiotracing mit ^{18}F-FDG teilen sich den bereits beschriebenen zellulären Aufnahmemechanismus des Tracers. Beim scRadiotracing wird nach *in vivo* Applikation die Glukoseaufnahme jedoch mit der Extraktion der Hirnzellen determiniert und der Tracer bleibt weiterhin für die Dauer des Versuchs in den Zellen messbar. Als Endergebnis des scRadiotracing reflektiert die quantifizierte Radioaktivität pro Einzelzelle demnach eine Momentaufnahme der zerebralen Glukoseaufnahme *in vivo*, zum Zeitpunkt der Hirnextraktion [19-21]. In zwei unabhängigen Studien zur Untersuchung der zellulären Tracerzuordnung konnte damit bereits unter Einsatz des grundlegenden Versuchsansatzes ein Zusammenhang zwischen Veränderungen des PET-Signals und des Glukosebedarfs während unterschiedlicher Aktivitätszustände von Mikrogliazellen nachgewiesen werden [19, 20].

Im Hinblick auf das Verständnis pathophysiologischer Mechanismen bei der Entstehung und Progression der AD ist die Erforschung des Metabolismus auf zellulärer Ebene in den Fokus gerückt. Dabei konnte bereits nachgewiesen werden, dass Gliazellen an der Pathogenese der AD beteiligt sind und maßgeblich die beobachteten PET-Signalveränderungen beeinflussen. Da dies insbesondere mit Abweichungen des mikroglialen Metabolismus einhergeht, ist es naheliegend, therapeutische Ansätze in ebendiesen Stoffwechselmechanismen zu ermitteln [20, 22, 23]. Allerdings bleibt die Untersuchung des zellulären Stoffwechsels *in vivo* herausfordernd, weshalb sich die meisten bisherigen Studien auf Zellkulturen und den Einsatz extrakorporaler, bioenergetischer *in vitro* Assays fokussierten. Unter hochkontrollierten Bedingungen erlauben einige dieser Verfahren die Quantifizierung sensitiver Parameter [24-27]. Jedoch sind gerade Mikrogliazellen dazu in der Lage, in Abhängigkeit von extrazellulären Signalen *in vivo*, wie etwa Adenosintriphosphat (ATP) bei lokaler Schädigung von Hirngewebe [28, 29] oder Apolipoproteine als

pathologische Rezeptorliganden [30], ihren Aktivitätszustand dynamisch zu modifizieren [31, 32]. Infolgedessen induzierte Prozesse, wie gesteigerte zelluläre Motilität durch morphologische Veränderungen [33] und angeregte Neurotransmittersynthese [34-36], resultieren in einem erhöhten Glukosebedarf für den Energiestoffwechsel. Diese Eigenschaft von Mikrogliazellen ist außerhalb des natürlichen Hirnmilieus kaum gewährleistet. Infolgedessen ist fraglich, ob die Ergebnisse reiner *in vitro* Studien die tatsächliche biologische Komplexität der *in vivo* Situation adäquat widerspiegeln können.

Ziel der vorliegenden Dissertationsschrift war es daher, unsere neuartige Methodik des scRadiotracing zur präklinischen *in vivo* Erforschung des zellulären Energiestoffwechsels von Hirnzellen zu erläutern und mit ihr die unmittelbare Vergleichbarkeit des mikroglialen Energiestoffwechsels *in vivo* mit *in vitro* zu untersuchen. Die vorliegende Arbeit ist im Kontext der Weiterentwicklung und Evaluierung des scRadiotracing zu verorten. Diese Methodik hat sich bereits in zahlreichen Studien und Kooperationsprojekten bewährt und zeichnet sich durch ein breites Spektrum an Einsatzmöglichkeiten aus [21, 37-44].

In nachfolgenden Abschnitten wird die der vorliegenden Dissertationsschrift zugrundeliegende Originalarbeit inhaltlich zusammengefasst. Der Zusammenhang zu multiplen assoziierten Projekten wird dargelegt und vor einer erweiterten Literaturübersicht in den wissenschaftlichen Kontext eingeordnet. Im Ausblick wird überdies die gegenwärtige und zukünftige Relevanz dieser Arbeit diskutiert und liefert Perspektiven auf die translationale Signifikanz für die Tiermedizin. Eine Publikationsliste aller im Rahmen dieser Disseration entstandenen Veröffentlichungen und Kooperationsprojekte, welche die hier vorgestellte Methodik implementiert haben, findet sich im Lebenslauf am Ende dieser Arbeit.

3. Untersuchung der Vergleichbarkeit der zellulären *in vivo* und *in vitro* Glukoseaufnahme mittels scRadiotracing

Kunte, S. T., Gnörich, J., Beumers, P., Bartos, L. M., Wagner, S., Wind-Mark, K., Holzgreve, A., Pötter, D., Werner, R. A., Ziegler, S., Albert, N. L., Colombo, A., Tahirovic, S., & Brendel, M. (2025). Distinct reduction in relative microglial glucose uptake compared to astrocytes and neurons upon isolation from the brain environment. Frontiers in cellular neuroscience, 19, 1572431. https://doi.org/10.3389/fncel.2025.1572431.

Aktuellen Erkenntnissen zufolge gelten molekulare Pathomechanismen, die eine Aktivierung von Mikrogliazellen und charakteristische zerebrale Stoffwechselsignaturen induzieren, als zentrale Marker zur Früherkennung neurodegenerativer Erkrankungen [45, 46]. Die Erfassung dieser metabolischen Alterationen *in vivo* bleibt bis dato jedoch eine Herausforderung, weshalb viele der bisherigen Studien auf extrakorporalen Untersuchungen an kultivierten Zellen und dem Einsatz bioenergetischer *in vitro* Assays basieren. Wesentlicher Aspekt in diesem Zusammenhang ist die hohe Anpassungsfähigkeit von Mikroglia, welche einen dynamischen Übergang zwischen komplexen Aktivitätszuständen ermöglicht [47, 48]. Dies stellt spezifische Anforderungen an die zelluläre Energiebereitstellung und wirft die Frage auf, ob Ergebnisse reiner *in vitro*-basierter Studien verlässlich sind. Daher wurde in dieser Studie, mit Fokus auf Mikrogliazellen, die Vergleichbarkeit der zellulären *in vivo* und *in vitro* ^{18}F-FDG-Traceraufnahme untersucht.

Der neuartige Ansatz des scRadiotracing ermöglichte dabei die Quantifizierung und Rückverfolgung des Tracers auf zellulärer Ebene als Momentaufnahme, normalisiert auf die gesamte zerebrale Glukoseaufnahme. Für diese Studie wurde das bewährte Versuchsprotokoll des scRadiotracing [20, 21, 37, 38, 40-43] erweitert. Das Ziel bestand darin, einen unmittelbaren Vergleich zu ermöglichen, indem an die Erfassung der zellulären Glukoseaufnahme *in vivo*, ein *in vitro* Inkubationsversuch mit denselben Zellen angeschlossen wurde.

Zunächst wurde Wild-typ Mäusen dafür *in vivo* der Radiotracer ^{18}F-FDG intravenös appliziert. Über Oberflächenmoleküle, CD11b für Mikroglia und ACSA-2 für Astrozyten, wurden die zerebralen Zellfraktionen mittels „immunomagnetischem cell sorting“ (MACS) isoliert – sowie die daraus resultierende nicht-Mikroglia-nicht-Astrozyten Fraktion. In einem unabhängigen Versuch wurde die Qualität der auf diese Weise angereicherten Zellfraktionen mittels Durchflusszytometrie (FACS), über den Grad der zellulären Reinheit validiert, wobei jeweils ein Wert von über 86% erreicht wurde.

Darüber hinaus konnten Neuronen mit einem Anteil von 79% als dominanter Zelltyp in der nicht-Mikroglia-nicht-Astrozyten Fraktion nachgewiesen werden. Im Folgenden wurde die Traceraufnahme pro Zellfraktion durch Messung der γ-Emission bestimmt und auf die Einzelzelle, durch Quantifizierung der absoluten Zellzahl mittels FACS, normalisiert. Dieses folglich relative System bietet den Vorteil, dass unabhängig von unter den Zellfraktionen gleichmäßig oder ungleichmäßig verteilten Zellverlusten, während einer selbst zeitintensiven Probenaufbereitung valide Daten generiert werden können. Auch wurde während der Versuche permanent kalter Puffer verwendet, um die Aktivität der mesophilen Glukose-6-Phosphatase in Hirnzellen [49-54], welche in der Lage wäre, Glukose-6-Phosphat in geringen Mengen zu hydrolysieren [55], auf ein Minimum zu limitieren. Anschließend wurden dieselben zuvor genannten Zellfraktionen einer exzessiven Inkubation in ^{18}F-FDG unterzogen. Nach Auswaschung des nicht-zellgebundenen Tracers erfolgte die analoge Quantifizierung der Glukoseaufnahme pro Einzelzelle.

Aufgrund der Tatsache, dass eine vorausgehende Untersuchung unserer Arbeitsgruppe eine Dosisabhängigkeit der zellulären ^{18}F-FDG-Aufnahme bewies [20], war es nicht möglich, die absolute Traceraufnahme nach *in vivo* Injektion, mit jener nach *in vitro* Inkubation zu vergleichen. Für eine korrekte Interpretation und Vergleichbarkeit der Daten war es daher notwendig, die Ergebnisse als Verhältnisse der Zellfraktionen zueinander zu betrachten. Isolierte Mikroglia zeigten dabei im Vergleich zu isolierten Astrozyten und nicht-Mikroglia-nicht-Astrozyten die bei Weitem höchste absolute Glukoseaufnahme nach *in vivo* Injektion. Auch nach der *in vitro* Inkubation wiesen Mikroglia die höchste absolute Traceraufnahme auf, wobei jedoch von *in vivo* zu *in vitro* eine deutliche Reduktion des Verhältnisses zu Astrozyten (von 50,4-fach auf 5,7-fach) und zu nicht-Mikroglia-nicht-Astrozyten (von 10,6-fach auf 1,7-fach) zu verzeichnen war.
Eine mögliche Beeinflussung der Ergebnisse durch die Injektion des Tracers wurde durch analoge *in vitro* Inkubation ohne vorausgehende *in vivo* Tracerinjektion experimentell überprüft und ausgeschlossen. Gleichermaßen konnte ein verzerrender Effekt durch Nüchternheit auf Mikroglia durch analoge Reproduktion der Versuche unter Verwendung von glukosefreiem Puffer ausgeschlossen werden.

Außerdem wurde ein Zellkulturversuch durchgeführt, um die relative Glukoseaufnahme *in vivo* (scRadiotracing), mit Zellen aus einem reinen *in vitro* Milieu

zu vergleichen. Im klaren Gegensatz zum scRadiotracing zeigten kultivierte Mikroglia im Vergleich zu kultivierten Neuronen und Astrozyten eine nur geringe ^{18}F-FDG-Aufnahme. Dabei übertraf die gemäß Literatur erwartet hohe Glukoseaufnahme von Neuronen [56, 57] jene von Astrozyten 8-fach und von Mikroglia 82-fach.

Bei diesem Zellkulturversuch und beim scRadiotracing, wurde der Verbrauch des für den Zellstoffwechsel notwendigen Substrats (Glukose) gemessen. Daneben gibt es viele weitere Methoden, die über verschiedene Parameter, wie die Erfassung der Metabolitenproduktion [27, 58-60], des Sauerstoffverbrauchs [24, 25, 61, 62] oder der Enzymexpression [63-65] eine Quantifizierung des zellulären Glukosemetabolismus ermöglichen. Hierbei muss jedoch differenziert werden, ob sich die Zellen zum Zeitpunkt der Messung noch in ihrem natürlichen Milieu befinden (*in vivo*), bereits extrahiert wurden (*ex vivo*) oder in der Zellkultur (*in vitro*) untersucht werden.

Die Ergebnisse dieser Studie demonstrieren, dass alleinige *in vitro* Messungen den zellulären *in vivo* Glukosestoffwechsel nicht akkurat widerspiegeln können. Relevant ist dies insbesondere bei der Grundlagenerforschung neurodegenerativer Erkrankungen wie AD mit multifaktorieller Ätiologie [66, 67], da derartige Methoden um die Nachahmung exakter *in vivo* Bedingungen limitiert sind [68]. Wie die vorausgehende Untersuchung unserer Arbeitsgruppe verdeutlichen konnte, werden Mikroglia im Rahmen von Amyloid-Erkrankungen durch diverse pathologische Prozesse beeinflusst und weisen daraufhin eine veränderte Rate ihres Glukosestoffwechsels auf [20]. Die neuartige Methodik des scRadiotracing komplementiert hingegen die präklinische zerebrale Bildgebung *in vivo* um eine suffiziente zelluläre Auflösung. Außerdem ermöglicht sie einfache Kombinierbarkeit mit anschließenden Untersuchungen des *ex vivo* Hirngewebes, beispielsweise mit Methoden der Transkriptomik und Proteomik.

Limitiert war unser Versuchsansatz um einige bisher ungeklärte Determinanten des scRadiotracing. Erstens, die während der mechanischen Homogenisierung des Gehirns verlorenen Zellfortsätze sind nicht quantifizierbar. Daher wird in dieser Studie nur die Glukoseaufnahme in Zellkörpern erfasst, welche zu einer Unterschätzung des Glukosestoffwechsels, insbesondere der Neuronen [16, 69, 70], führen könnte. Zweitens, ^{18}F-FDG könnte während des Versuchsablaufs aus beschädigten Zellen entweichen und anschließend von intakten Zellen wiederaufgenommen werden. Drittens, die Traceraufnahme in Hirnzellen ist abhängig von der Passage der Blut-Hirn-

Schranke, welche durch die Dosis-abhängige interindividuelle Hypotension [71] des verwendeten Inhalationsanästhetikums beeinflusst sein könnte.

Zusammengefasst lässt sich konstatieren, dass Mikrogliazellen relativ zu den anderen untersuchten Hirnzellen, im direkten Vergleich *in vivo* mit *in vitro*, eine deutlich reduzierte Glukoseaufnahme zeigen. Im Rahmen einer Erforschung des mikroglialen Energiestoffwechsels, unter Einsatz reiner *in vitro* Methode, sollten diese Erkenntnisse bei der Interpretation der Daten berücksichtigt werden. Dahingegen erlauben einige Methoden *in vivo* und *ex vivo* Anwendbarkeit. Unter jenen sticht scRadiotracing durch die Ermöglichung der zuvor nicht vorhandenen zellulären Auflösung hervor und vereinfacht die umfangreiche Untersuchung des *in vivo* Glukosemetabolismus durch Implementierbarkeit in multimodale Studienkonzepte.

4. Originalarbeit

4.1 **Kunte, S. T.**, Gnörich, J., Beumers, P., Bartos, L. M., Wagner, S., Wind-Mark, K., Holzgreve, A., Pötter, D., Werner, R. A., Ziegler, S., Albert, N. L., Colombo, A., Tahirovic, S., & Brendel, M. (2025). Distinct reduction in relative microglial glucose uptake compared to astrocytes and neurons upon isolation from the brain environment. *Frontiers in cellular neuroscience*, *19*, 1572431. https://doi.org/10.3389/fncel.2025.1572431.

frontiers | Frontiers in Cellular Neuroscience

TYPE Original Research
PUBLISHED 15 September 2025
DOI 10.3389/fncel.2025.1572431

OPEN ACCESS

EDITED BY
Zhe Jin,
Uppsala University, Sweden

REVIEWED BY
Xuyan Jin,
Massachusetts General Hospital and Harvard Medical School, United States
Virginia Mela,
Andalusian Public Foundation for Malaga Research in Biomedicine and Health (FIMABIS), Spain

*CORRESPONDENCE
Matthias Brendel
✉ Matthias.Brendel@med.uni-muenchen.de

RECEIVED 19 February 2025
ACCEPTED 15 August 2025
PUBLISHED 15 September 2025

CITATION
Kunte ST, Gnörich J, Beumers P, Bartos LM, Wagner S, Wind-Mark K, Holzgreve A, Pötter D, Werner RA, Ziegler S, Albert NL, Colombo A, Tahirovic S and Brendel M (2025) Distinct reduction in relative microglial glucose uptake compared to astrocytes and neurons upon isolation from the brain environment.
Front. Cell. Neurosci. 19:1572431.
doi: 10.3389/fncel.2025.1572431

Distinct reduction in relative microglial glucose uptake compared to astrocytes and neurons upon isolation from the brain environment

Sebastian T. Kunte[1,2], Johannes Gnörich[1,3], Philipp Beumers[1], Laura M. Bartos[1], Stephan Wagner[1], Karin Wind-Mark[1], Adrien Holzgreve[1], Dennis Pötter[1], Rudolf A. Werner[1,4], Sibylle Ziegler[1,3], Nathalie L. Albert[1,5,6], Alessio Colombo[7], Sabina Tahirovic[7] and Matthias Brendel[1,3,5,6,7]*

[1]Department of Nuclear Medicine, LMU University Hospital, Munich, Germany, [2]Section of Clinical and Comparative Neuropathology, Institute for Veterinary Pathology, Center for Clinical Veterinary Medicine, LMU, Munich, Germany, [3]Munich Cluster for Systems Neurology (SyNergy), University of Munich, Munich, Germany, [4]Russell H. Morgan Department of Radiology and Radiological Sciences, Johns Hopkins School of Medicine, Baltimore, MD, United States, [5]German Cancer Consortium (DKTK), Partner Site Munich, German Cancer Research Center (DKFZ), Heidelberg, Germany, [6]Bavarian Cancer Research Center (BZKF), Erlangen, Germany, [7]German Center for Neurodegenerative Diseases (DZNE) Munich, Munich, Germany

Introduction: Microglial energy metabolism has gained attention for the treatment of neurodegenerative diseases. *In vitro* methods provide important insights; however, it remains unclear whether the metabolism of highly motile microglia is preserved outside their regular environment. Therefore, we directly compared the microglial glucose uptake *in vivo* and in vitro in mice.

Methods: Microglia and astrocytes were isolated from the brain using immunomagnetic cell sorting following [^{18}F]FDG injection in living mice, followed by gamma and single-cell radiotracing (scRadiotracing). Enriched cell fractions were incubated with excess [^{18}F]FDG (50,000-fold) *in vivo*, washed, and measured equivalently. For all fractions, radioactivity per cell was normalized to the injected or incubated radioactivity, and ratios of microglialuptake were calculated relative to astrocytes and the microglia/astrocyte-negative fraction. The experiment was repeated using a glucose-free buffer and validated by in vitro incubation without prior in vivo [^{18}F]FDG injection to exclude the influence of fasting and glucose injection.

Results: scRadiotracing results were compared against cell culture [^{18}F]-FDG incubation. The in vivo glucose uptake of microglia was higher when compared to astrocytes (50.4-fold, $p < 0.0001$) and non-microglia/ non-astrocyte cells (10.6-fold, $p < 0.0001$). Microglia still exhibited the highest glucose uptake in vitro, but with a distinct reduction in microglia-to-astrocyte (5.7-fold, $p < 0.0015$) and microglia-to-microglia/astrocyte-negative ratios (1.7 fold, $p < 0.0001$). Fasting and in vitro incubation were used to validate the results. Cell culture indicated low microglial uptake compared to that in neurons (1:100) or astrocytes (1:10).

Discussion: Compared to astrocytes and other cells, microglia show a distinct reduction in uptake in vitro compared to in vivo uptake. Our results emphasize that in vitro experiments should be interpreted with caution when studying microglial energy metabolism.

KEYWORDS

microglia, glucose uptake, *in vivo*, *in vitro*, scRadiotracing

1 Introduction

Microglial activation and characteristic metabolic patterns have been widely recognized as hallmarks of neurodegenerative diseases such as Alzheimer's disease (AD) (Gao et al., 2019; Rauchmann et al., 2022). These alterations may substantially precede the manifestation of pathognomonic cerebral alterations, i.e., the presence of neurofibrillary tangles or senile plaques (Bubber et al., 2005; Mattson, 2004; Moreira et al., 2007; Wallace, 2005). Therefore, fundamental knowledge of changes in cellular metabolism is crucial to facilitate the recognition of disease onset at an early stage (Mosconi, 2005). Additionally, future investigations on pivotal microglial functions and metabolic interactions between resident cells of the brain may yield novel therapeutic approaches (Fumagalli et al., 2018; Jung et al., 2025). In this regard, the assessment of *in vivo* microglial metabolism remains challenging, thereby hindering the progress in understanding the observed metabolism-associated biomechanisms. The majority of studies conducted hitherto, thus, have focused on cultured cells and Seahorse assay-based bioenergetic analysis. The Seahorse assay facilitates the quantification of the oxygen consumption rate (OCR) as a measure of mitochondrial respiration and the extracellular acidification rate (ECAR), indicating glycolysis (Zhang et al., 2021). In addition, single-cell RNA sequencing (scRNA-seq) analysis captures changes in key metabolic enzymes that influence changes in cellular energy metabolism (Hrovatin et al., 2022). However, microglia are capable of rapidly shifting between activation states in response to their environment. Consequently, they need to specialize their metabolic demands to suit these distinct states, such as resting, surveillance, or activation (Bernier et al., 2020; Orihuela et al., 2016). Several studies uncovered distinct expression patterns of key metabolic enzymes and transporters in microglia, dependent on cellular activation, by scRNA-seq and protein measurements (Xiang et al., 2021; Hammond et al., 2019; Hrovatin et al., 2022; Olah et al., 2020; Zhang et al., 2014).

However, microglial energy metabolism assays that use a snapshot several hours after isolation of microglia from the regular brain environment may still experience bias due to changes in cellular energy demand and gene expression. Thus, although these assays are highly valuable for comparison of microglial energy metabolism under different conditions, there is a strong need to investigate alterations in microglial energy metabolism *in vivo* and *in vitro*. Radioactive 2-Fluor-2-desoxy-D-glucose (i.e., [^{18}F]FDG) facilitates the assessment of cellular glucose uptake at the time of tracer injection *in vivo* because FDG is trapped inside the cell upon phosphorylation and is not further metabolized. Importantly, this methodology can also be used in conjunction with PET (Minoshima et al., 2022) or autoradiography (Sokoloff et al., 1977) to generate a snapshot of glucose uptake during a certain task. Moreover, we and others recently established workflows to track this tracer uptake at cellular resolution (Bartos et al., 2022; Choi et al., 2021; Xiang et al., 2021). In particular, two independent studies observed a significant increase in microglial glucose uptake in mouse models of amyloidosis when compared to wild-type mice, which indicated an altered energy demand at different microglial activation states (Xiang et al., 2021; Choi et al., 2021).

To compare glucose uptake by microglia *in vivo* and *in vitro*, we extended our established workflow and performed a head-to-head comparison of tracer uptake per cell between *in vivo* [^{18}F]FDG injection in living mice and subsequent *in vitro* incubation of the same *ex vivo* isolated cells with excessive [^{18}F]FDG. Furthermore, we performed cross-validation of our results using a glucose-free buffer and *in vitro* application without prior *in vivo* [^{18}F]FDG injection. Finally, we compared microglial glucose uptake in cell cultures with that by microglia in a regular brain environment.

2 Materials and methods

2.1 Experimental setup and study design

All animal experiments were performed with the approval of the local animal care committee of the Government of Upper Bavaria (Regierung von Oberbayern) and in accordance with the National Guidelines for the Protection of Animals. The animals used for the experiments were monitored by a veterinarian. Experiments were executed in compliance with the ARRIVE (Animal Research: Reporting of *In Vivo* Experiments) guidelines and in accordance with the U. K. Animals (Scientific Procedures) Act, 1986, and associated guidelines, EU Directive 2010/63/EU for animal experiments. Animals were kept in a temperature- and humidity-controlled environment with a 12-h light–dark cycle, with unrestricted access to food and water. For this study, a total of female (n = 20) wild-type mice (C57BL6) at an average age of 3.4 ± 0.4 months underwent single-cell Radiotracing (scRadiotracing) (Bartos et al., 2022; Xiang et al., 2021) for direct comparison of *in vivo* and *in vitro* glucose uptake of microglia. Figure 1 illustrates the study design, study groups, and workflow, which included tracer injection, brain removal, generation of single-cell suspension, immunomagnetic cell sorting (MACS), gamma emission counting, and flow cytometry. Sample sizes were determined based on previous experience with the workflow (Bartos et al., 2024a; Dinkel et al., 2024; Gnörich et al., 2023; Xiang et al., 2021; Slemann et al., 2024; Bartos et al., 2023; Bartos et al., 2024b).

Tracer uptake upon *in vivo* [^{18}F]FDG injection, followed by incubation with excess [^{18}F]FDG (50,000-fold), was measured in mice (n = 16). Using catheters, the tracer was injected into the ventral tail vein, followed by flushing to ensure complete bolus application (Table 1). The mice were separated from their access to food for >3 h before tracer injection. Anesthesia was performed with 1.5% isoflurane delivered at 1.5 L/min O_2. To consider the influence of cell fasting, a buffer containing glucose (1,000 mg/L) and a glucose-free buffer were used for each mouse (n = 8).

For cross-validation, another mouse (n = 4) underwent *in vitro* [^{18}F]FDG incubation without prior *in vivo* [^{18}F]FDG injection after the generation of the single-cell suspension (glucose-free buffer).

Moreover, we measured the glucose uptake of cultured microglia, astrocytes, and neurons after [^{18}F]FDG incubation for comparison with uptake values from scRadiotracing (Bartos et al., 2022).

10.3389/fncel.2025.1572431

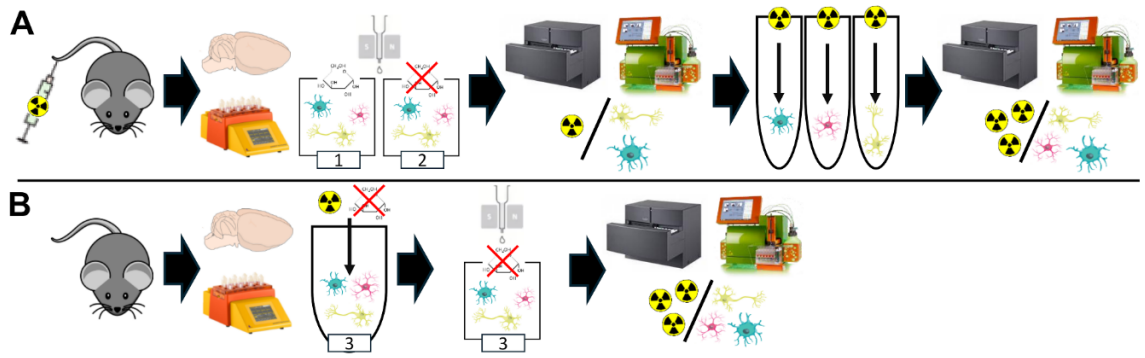

FIGURE 1
Experimental setup for head-to-head comparison of *in vivo* and *in vitro* glucose uptake using a modified scRadiotracing protocol. **(A)** The experimental workflow of an extended scRadiotracing protocol enables direct comparison of *in vivo* and *in vitro* glucose uptake (study group 1, Table 1). *In vivo* [^{18}F]FDG application was followed by brain dissociation in a buffer containing glucose, magnetic-activated cell sorting, and determination of radioactivity per cell body. Radioactivity per cell body was equivalently determined after subsequent *in vitro* incubation with excessive [^{18}F]FDG. To investigate the influence of strict fasting on cells, a glucose-free buffer was used equally throughout the workflow (study group 2, Table 1). **(B)** To exclude potential effects of *in vivo* [^{18}F]FDG application prior to *in vitro* incubation, the scRadiotracing workflow was modified for *in vitro* incubation without prior *in vivo* [^{18}F]FDG injection (study group 3, Table 1). After brain extraction and dissociation, *in vitro* incubation was performed, followed by magnetic-activated cell sorting and determination of the radioactivity per cell body. Glucose-free buffer was used throughout the workflow.

TABLE 1 **Summary of study groups.**

Method	Group	Buffer	Mouse model	Animals (n)	Sex	Age (months)	Body weight (g)	Injected dose (MBq)	Incubation dose (MBq)
In vivo + *In vitro*	1	glucose	wild-type	8	f	4.0	23.3 ± 1.0	15.0 ± 3.3	8.5 ± 0.5
	2	glucose-free	wild-type	8	f	3.5	21.3 ± 1.3	16.2 ± 1.6	2.9 ± 0.5
In vitro validation	3	glucose-free	wild-type	4	f	3.0	20.5 ± 0.6	/	7.3 ± 0.4
Cell culture	4	glucose-free	/	11–12 per cell type	f	/	/	/	0.1

Brief overview of key determinants defining the major study groups in the experimental setup of this study. f = female, MBq = megabecquerel.

2.2 Preparation of single-cell suspensions

Using the Adult Brain Dissociation Kit, mouse, and rat (Miltenyi Biotec, 130–107-677), single-cell suspensions were prepared according to the manufacturer's instructions.

After dissection, adult mouse brains were briefly washed in cold phosphate-buffered saline (PBS) and cut into sagittal slices ($n = 8$). Brain dissociation was performed in enzyme mixes 1 and 2 using a gentleMACS™ Octo Dissociator with Heaters (Miltenyi Biotec, 130–096-427). The resulting brain homogenates were then applied onto pre-moistened MACS® SmartStrainers (70 µm) and washed by rinsing with 2 × 10 mL of PBS. After centrifugation at 300 × g for 10 min at 4 °C, the pellets were resuspended in PBS and Debris Removal Solution. Cold PBS was gently overlaid. After centrifugation at 3,000 × *g* for 10 min at 4 °C, the top two phases were discarded. The cell pellets were washed and resuspended in 1 mL of Red Blood Cell Removal Solution (10x). After incubation for 10 min in the dark in a refrigerator at 4 °C, cell pellets were washed with cold PBS-0.5% BSA buffer and collected for positive isolation of microglia and astrocytes via magnetic-activated cell sorting (Bartos et al., 2022; Xiang et al., 2021).

To consider the influence of fasting, this preparation process was performed with PBS buffer containing glucose for wild-type mice ($n = 8$) and with glucose-free buffer for wild-type mice ($n = 8 + 4$).

2.3 Isolation of microglia

The isolation process of microglia was performed by immunomagnetic cell sorting following the manufacturer's instructions for CD11b (microglia) MicroBeads (Miltenyi Biotec, 130–093-634) for up to 10^7 cells.

Prepared single-cell pellets were resuspended in 90 µL of cold PBS-0.5% BSA buffer and labeled with 10 µL of CD11b (Microglia) MicroBeads (Miltenyi Biotec, 130–093-634). After incubation for 15 min in the dark in a refrigerator at 4 °C, the cells were washed and resuspended in 500 µL of PBS-0.5% BSA buffer. LS columns (Miltenyi Biotec, 130–042-401) were prepared by rinsing with 3 mL of PBS-0.5% BSA buffer, followed by application of the cell suspensions onto the columns. The columns were washed with 3 × 3 mL of PBS-0.5% BSA buffer. The flow-through containing unlabeled cells was collected as the microglia-depleted fraction. Labeled cells were collected by flushing the columns with 5 mL of PBS-0.5% BSA buffer and were considered microglia-enriched fractions. Microglia-enriched fractions were analyzed using gamma emission recording (radioactivity per pellet, see Section 2.6) and flow cytometry (cell count and purity per pellet, see Section 2.7). Glucose-enriched or glucose-free buffers were maintained as described in Section 2.2.

2.4 Isolation of astrocytes

To isolate astrocytes by immunomagnetic cell sorting, the Anti-ACSA2 MicroBead Kit (Miltenyi Biotec, 130–097-678) was used according to the manufacturer's instructions for up to 10^7 total cells.

The flow-through fractions containing unlabeled cells negative for CD11b from the microglial isolation process were resuspended in 80 µL of cold AstroMACS Separation Buffer (Miltenyi Biotec, 130–117-336) and labeled with 10 µL of FcR Blocking Reagent. After incubation for 10 min in the dark in a refrigerator, 10 µL of Anti-ACSA2 MicroBeads was added, followed by incubation for 15 min in a refrigerator. The cells were washed and applied to pre-moistened LS columns. The columns were washed with 3 × 3 mL of AstroMACS Separation Buffer. The flow-through containing unlabeled cells was collected as microglia- and astrocyte-depleted fractions. The predominant proportion of neuronal cells in this fraction (79.5 ± 5.0%) was validated by CD90.2 staining (see Section 2.7). Labeled cells were collected by flushing the columns with 5 mL of AstroMACS Separation Buffer and were considered as astrocyte-enriched fractions. Microglia- and astrocyte-depleted fractions, as well as astrocyte-enriched fractions, were analyzed using gamma emission recording (radioactivity per pellet, see Section 2.6) and flow cytometry (cell count and purity per pellet, see Section 2.7). Glucose-enriched or glucose-free buffers were maintained as described in Section 2.2. Validation of ACSA-2 sorting of astrocytes was validated via GFAP elsewhere (Xiang et al., 2021).

2.5 *In vitro* incubation

For a direct comparison of *in vivo* and *in vitro* glucose uptake, all *ex vivo* isolated cell fractions were resuspended in 1 mL PBS and incubated *in vitro* with excess [^{18}F]FDG (50,000-fold; radioactivity used for incubation relative to radioactivity in the cell pellet). After 30 min of uptake in the dark, the samples were washed to remove non-cellular-bound tracers. Then, 5 mL of cold PBS was added, followed by centrifugation at 400 × g for 5 min at 4 °C. This washing procedure was repeated five times to ensure the exclusion of non-cellular [^{18}F]FDG from the measured probes.

Glucose-enriched and glucose-free buffers were maintained as described in Section 2.2. To eliminate the confounding effects of the *in vivo* injection, the procedure was repeated by *in vitro* incubation without prior *in vivo* [^{18}F]FDG injection in wild-type mice (n = 4). *In vitro* incubation was performed directly after the preparation of single-cell suspensions. Non-cellular bound [^{18}F]FDG was removed during >5 washing steps during the isolation process for microglia and astrocytes.

2.6 Gamma emission measurements

To measure the radioactivity concentrations of the cell pellets, gamma emission recordings were performed using a highly sensitive gamma counter (Hidex AMG Automatic Gamma Counter, Mainz, Germany). Each probe was measured for 1 min. The results of cell sorting after the *in vivo* injection were normalized to the activity in the whole brain, including decay correction to the time of tracer injection. Results of cell sorting after *in vitro* incubation were normalized to the amount of radioactivity used for incubation.

2.7 Sample analysis by flow cytometry

Flow cytometry was performed to analyze the fraction purity and cell count after *in vivo* tracer injection and *in vitro* incubation.

The cell pellets were resuspended in 100 µL cold PBS. Microglia were stained with 1.5 µL of CD11b Antibody, linked with VioBlue® (Miltenyi Biotec, 130–113-810) or APC (BioLegend®, 101,212). Astrocytes were stained with 1.5 µL of ACSA2 Antibody, linked with APC (Miltenyi Biotec, 130–116-142) or PE-Vio® 615 (Miltenyi Biotec, 130–116-249). After incubation for 10 min in the dark in a refrigerator, the incubation was terminated by adding 1.5 mL of PBS. The samples were analyzed by flow cytometry using a MACSQuant® Analyzer 10 Flow Cytometer (Miltenyi Biotec, 130–096-343; Figure 2A). Cell count represents the number of singlets per fraction. Purity was defined as the percentage of CD11b-positive microglia or ACSA2-positive astrocytes per enriched cell fraction. Purity of the microglia- and astrocyte-depleted fraction was determined by CD11b- and ACSA2-negativity, and the proportion of neurons was cross-validated by CD90.2 (Thy-1.2 Antibody, Invitrogen, 25–0902-81; Figure 2B) staining using independent samples that underwent equal processing. CD11b-VioBlue® and APC-ACSA2 are presented throughout the manuscript.

2.8 Cell culture

Relative [^{18}F]FDG uptake by cells in an exclusive *in vitro* environment was measured to compare the cell culture results with the uptake of cells isolated from a regular brain environment (see Sections 2.2–2.6, 2.7) performed in buffer without glucose. Primary embryonic hippocampal neurons and astrocytes were isolated from embryonic day 18 CD rats (Charles River), as previously described (Kaech and Banker, 2006; Montagna et al., 2019; Willem et al., 2015), and cultured in a humidified 5% CO_2 incubator at 37 °C. Hippocampal neurons were plated onto 6-well plates containing glass coverslips coated with 1 mg/mL poly-L-lysine and maintained for 10 days in Neurobasal medium supplemented with 2% B27 and 0.5 mM L-glutamine (all from Invitrogen). Astrocytes were plated in untreated T-75 tissue culture flasks (Nunc) and cultured in minimal essential medium (Gibco) supplemented with horse serum (MEM-HS) until they reached approximately 80% confluency, when the cells were passaged and used 2 days after the first or second passaging. Postnatal P7 mouse microglia were isolated and cultured as previously described (Dinkel et al., 2024).

Wells were prepared with either microglia or astrocytes (n = 75,000 and 600 µL DMEM-F12 (Gibco) supplemented with 10% FBS and 1% penicillin/streptomycin (Gibco) medium per well) or neurons (n = 75,000 and 600 µL NEUROBASAL medium per well) and incubated for 60 min at 37 °C. After incubation for 120 min with [^{18}F]FDG (100 kBq in 200 µL per well), the medium and tracers were removed. To eliminate non-cellular-bound tracers, the wells were washed with 800 µL of PBS. The cells were then incubated twice with 800 µL NaOH for 10 min and transferred to collection tubes. Cellular radioactivity was measured by gamma counting (see Section 2.6). Radioactivity values (counts per minute; CPM) were normalized to the measured reference activity (CPM/

10.3389/fncel.2025.1572431

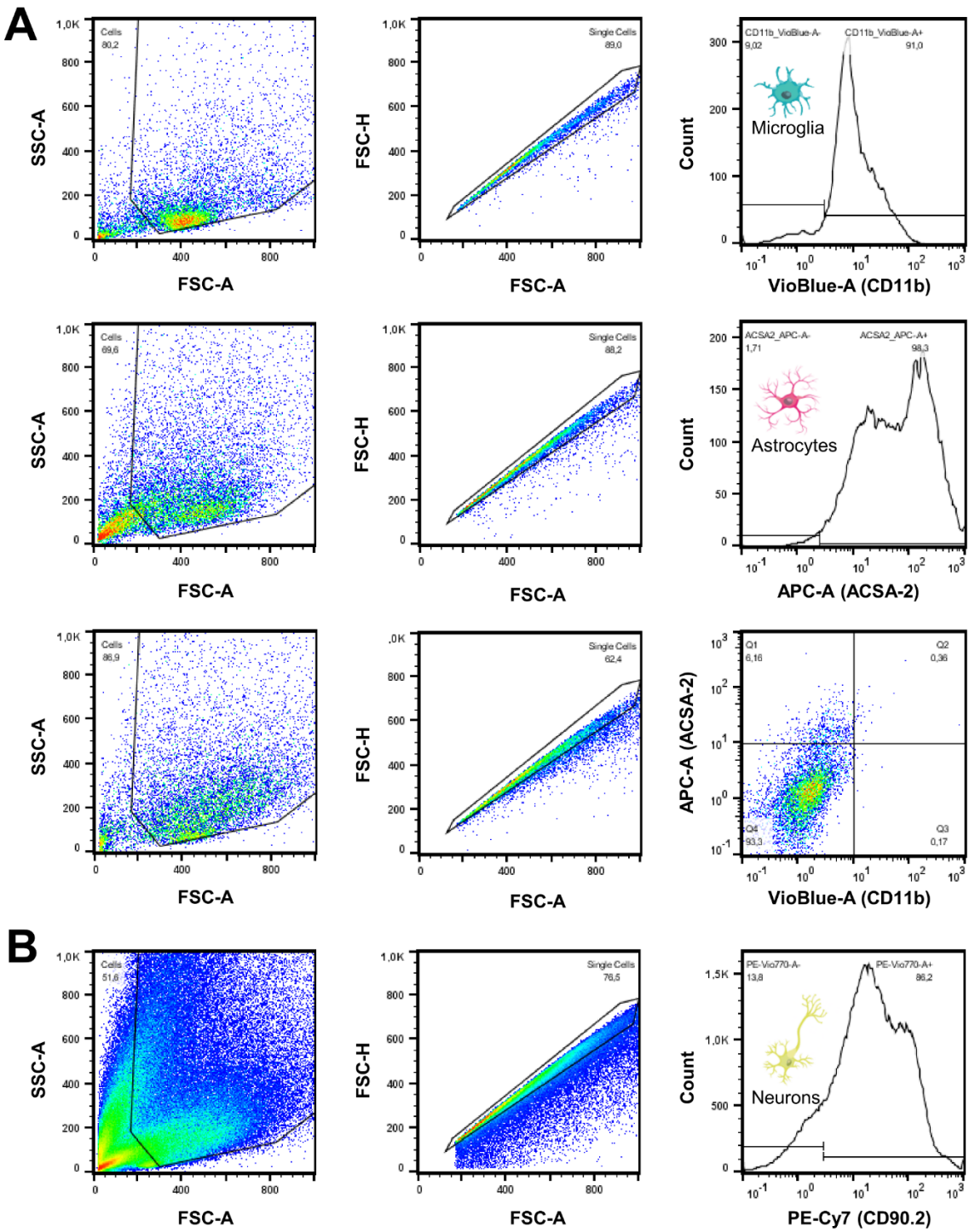

FIGURE 2
Quality measures of cell sorting procedures show excellent purity of enriched cell fractions. **(A)** Following the gating strategy, validation of purity and cell counting of isolated cell fractions (CD11b+, ACSA2+, CD11b-/ACSA2-) was executed by FACS analysis. As shown in the stagger-offset histograms, microglial and astrocytic fractions were collected with robust purity. Non-microglia/non-astrocyte cell fraction gates were defined as CD11b and ACSA2 negative. **(B)** The high proportion of neurons in non-microglia/non-astrocyte cell fractions was cross-validated using CD90.2 in independent samples. A high proportion of neurons was identified after manual microglia and astrocyte depletion and after depletion using an AutoMACS® Pro Separator.

CPMref), including decay correction to the time of tracer incubation as a readout of the percentage uptake. Furthermore, cellular radioactivity was normalized to the cell number as uptake per cell (CPM/cell).

2.9 Statistical analysis

IBM® SPSS® Statistics (IBM, V28.0) and GraphPad Prism (V9.4) were used for the statistical analysis and visualization. A p-value of < 0.05 was considered significant.

For all cell fractions, radioactivity per cell was calculated and normalized to injected or incubated radioactivity, and ratios of glucose uptake in microglia cells were calculated relative to the uptake in astrocytes and the microglia/astrocyte-negative fraction.

Kolmogorov–Smirnov and Shapiro–Wilk tests were used to confirm the data of each group (see Section 2.1; Figure 1) on normal distribution. A paired Student's t-test was used to compare the glucose uptake of microglia-to-astrocyte, microglia-to-microglia/astrocyte-negative, and astrocyte-to-microglia/astrocyte-negative cell ratios between *in vivo* injection and *in vitro* incubation (see 3.1). Unpaired Student's t-tests were used to compare the absolute glucose uptake values between single microglia, single astrocytes, and non-microglia/non-astrocyte cells (see Section 3.2). A one-way ANOVA was used to compare glucose uptake by microglia, astrocytes, and neurons in Section 3.3. All data are presented as mean ± SD. A *post hoc* power analysis (two-tailed t-test, $\alpha = 0.05$, power = 80%) indicated that the study was sufficiently powered to detect the actual effect sizes (all Cohen's $d > 1.16$) for the comparison of *in vivo* and *in vitro* FDG uptake as well as the influence of fasting (with $n = 8$ samples per group). For the cell culture experiment, the required effect size of Cohen's $d > 0.55$ (with $n = 11–12$ samples per group) to detect significant differences at a power of 80% and $\alpha = 0.05$ (one-way ANOVA) was met.

3 Results

3.1 Distinct relative reduction of microglial glucose uptake when isolated from the brain environment

First, we aimed to compare the glucose uptake of microglia in the regular brain environment after *in vivo* tracer injection head-to-head with the glucose uptake of the same cells *in vitro* using scRadiotracing. It was hypothesized that microglia display reduced relative glucose uptake when comparing *in vitro* incubation with *in vivo* glucose uptake. Enrichment by MACS facilitated the high purity of microglia (86.4% ± 3.3%), astrocytes (94.2% ± 2.4%), and microglia- and astrocyte-depleted fractions (92.6% ± 1.5%, Figure 2A). Neurons were the predominant cell type in the CD11b- and ACSA2-negative fraction, as determined by CD90.2 (79.5% ± 5.0%, Figure 2B). As expected, the isolation procedure resulted in enrichment of cell bodies, whereas cell processes, axons, and synapses were lost.

After *in vivo* [^{18}F]FDG injection, single microglial cell bodies showed higher glucose uptake than single astrocyte cell bodies (50.4-fold, $p < 0.0001$) and single non-microglia/non-astrocyte cell bodies (10.6-fold, $p < 0.0001$). Microglial cell bodies still showed the highest glucose uptake *in vitro*, but we observed a distinct reduction in the microglia-to-astrocyte ratio (5.7 vs. 50.4, $p = 0.0015$) and microglia-to-microglia/astrocyte-negative cell ratio (1.7 vs. 10.6, $p < 0.0001$). Glucose uptake *in vivo* was lower per astrocyte cell body than in non-microglia/non-astrocyte cell bodies (0.2-fold, $p < 0.0001$), and this ratio did not change significantly *in vitro* (0.4 vs. 0.2, $p = 0.089$, Figure 3).

3.2 Strict fasting does not affect microglial glucose uptake but increases astrocytic glucose uptake

To consider the influence of strict fasting on cells, the experiment was repeated equivalently with a glucose-free buffer (Figure 3). The mice were fasted for >3 h before tracer injection under both conditions. Subsequently, to investigate the potential effects of *in vivo* [^{18}F]FDG injection, the experiment was validated using *in vitro* incubation without prior *in vivo* [^{18}F]FDG injection. It was presumed that microglial glucose uptake was not influenced by fasting or prior *in vivo* [^{18}F]FDG injection.

No significant change in glucose uptake per microglial cell body was observed when comparing glucose-free buffer with buffer containing glucose *in vivo* (1.61E-6% vs. 1.33E-6%, $p = 0.353$) or *in vitro* (1.93E-3% vs. 1.83E-3%, $p = 0.845$; Figure 4). Astrocytic glucose uptake per cell body was higher in the glucose-free buffer than in the buffer containing glucose *in vivo* (3.44E-8% vs. 5.52E-8%, $p = 0.0007$) and *in vitro* (6.85E-4% vs. 1.66E-3%, $p = 0.0082$; Figure 4). Single non-microglia/non-astrocyte cell bodies showed no significant change in glucose uptake compared with glucose-free buffer with buffer containing glucose (*in vivo:* 1.61E-7% vs. 1.43E-7%, $p = 0.369$; *in vitro*: 1.52E-3% vs. 3.48E-3%, $p = 0.081$). As a consequence, glucose-free buffer led to a reduction in the microglia-to-astrocyte ratio after *in vivo* injection (ratio 50.4 vs. 24.2, $p < 0.0037$) and *in vitro* (ratio 5.7 vs. 0.9, $p = 0.035$) compared to the buffer containing glucose. In contrast, the microglia-to-microglia/astrocyte-negative cell ratio (*in vivo:* ratio 10.6 vs. 9.1, $p = 0.449$; *in vitro*: ratio 1.7 vs. 0.8, $p = 0.057$) remained similar, whereas the astrocyte-to-microglia/astrocyte-negative (*in vivo:* ratio 0.2 vs. 0.4, $p < 0.0026$; *in vitro*: ratio 0.4 vs. 1.0, $p = 0.0028$) increased significantly.

Single microglia (−9%, 1.67E-3% vs. 1.83E-3%, $p = 0.784$) did not show significant changes in glucose uptake after *in vitro* incubation when compared to *in vitro* incubation after *in vivo* injection. In contrast, single astrocytes (+66%, 2.53E-3% vs. 1.66E-3%, $p = 0.0003$) indicated an increase in [^{18}F]FDG uptake.

In summary, cross-validation experiments confirmed a reduction in microglial glucose uptake *in vitro* compared to *in vivo* applications. Astrocyte glucose uptake may have a higher sensitivity to low amounts of glucose than glucose uptake by microglia.

3.3 Relative glucose uptake of neurons, astrocytes, and microglia in cell culture differs from relative glucose uptake in the regular brain environment

Finally, we performed a cell culture experiment to compare the relative [^{18}F]FDG uptake of cells isolated from the normal brain environment with that of cells in a pure *in vitro* environment

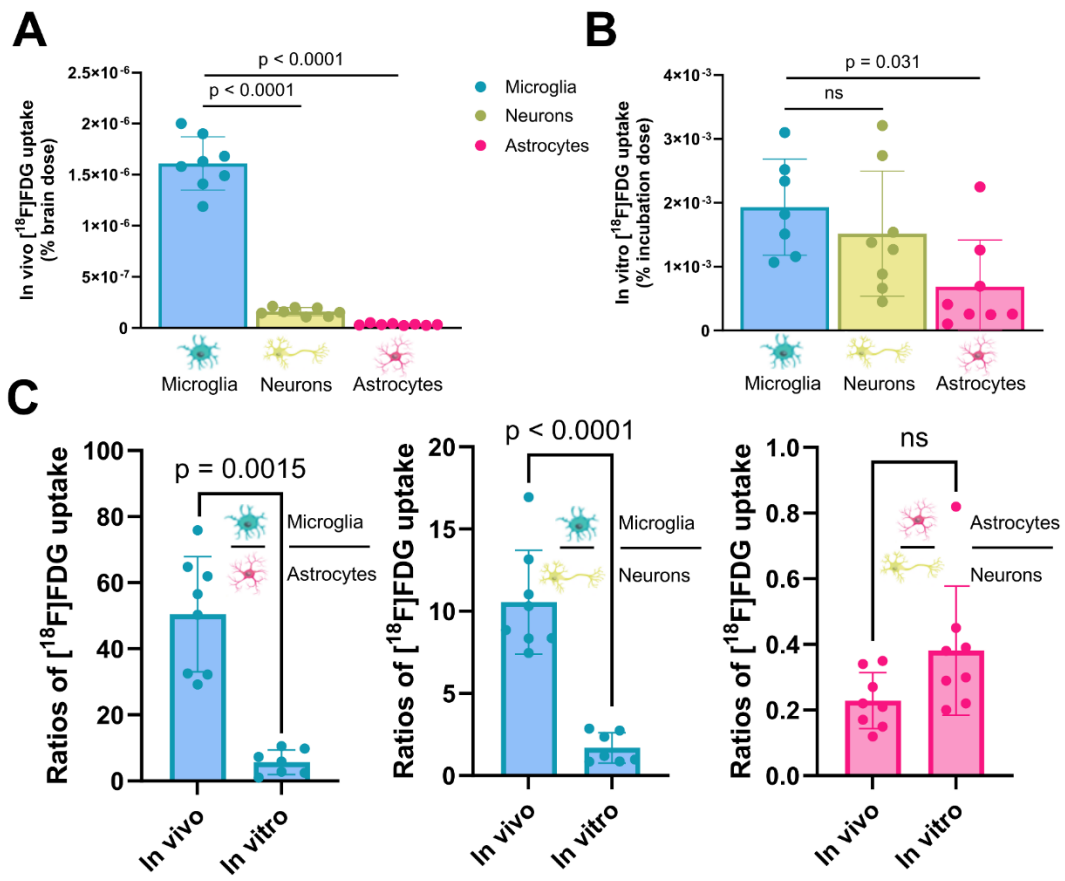

FIGURE 3
Microglia exhibit a distinct relative reduction in glucose uptake when isolated from a regular brain environment. **(A)** Direct comparison of in vivo [18F]FDG uptake among microglia, neurons, and astrocytes after normalization to whole-brain [^{18}F]FDG uptake. **(B)** Direct comparison of *in vitro* [^{18}F]FDG uptake among microglia, neurons, and astrocytes after normalization to the incubation dose. **(C)** Cell-type-specific ratios of [^{18}F]FDG uptake in a direct comparison between *in vivo* and *in vitro* environments. After calculating the radioactivity per single cell, *in vivo* and *in vitro* microglia-to-astrocyte (left plot), microglia-to-microglia/astrocyte-negative (middle plot), and astrocyte-to-microglia/astrocyte-negative (right plot) cell ratios were compared.

(Figure 5). The rationale of this experiment was to compare the *in vitro* conditions shortly after brain dissociation (sections 3.1 and 3.2) with a pure *in vitro* environment. Neurons of the cell culture indicated the highest [^{18}F]FDG uptake (10.44 ± 2.04 CPM/cell; cell fraction uptake: 21.50 ± 4.19%), exceeding astrocytes (1.25 ± 0.10 CPM/cell; cell fraction uptake: 2.57 ± 0.22%) by 8-fold ($p < 0.0001$) and microglia (0.13 ± 0.02 CPM/cell; cell fraction uptake: 0.26 ± 0.05%) by 82-fold ($p < 0.0001$).

4 Discussion

To study microglial glucose uptake relative to other cells of the brain in the comparison of a regular brain environment with an *in vitro* environment, we measured cellular glucose uptake in wild-type mice after *in vivo* [^{18}F]FDG injection and subsequent *in vitro* incubation by scRadiotracing (Bartos et al., 2022). This novel approach provides a unique opportunity for direct head-to-head comparisons of glucose uptake in the same cells *in vivo* and *in vitro*.

Single microglial cell bodies exhibited higher glucose uptake after *in vivo* injection when compared to cell bodies of single astrocytes and cell bodies of single non-microglia/non-astrocyte cells, i.e., neurons, which was one of the main results of our previous study (Xiang et al., 2021). Despite still showing the highest glucose uptake after excessive *in vitro* [^{18}F]FDG incubation, the microglia-to-astrocyte and microglia-to-microglia/astrocyte-negative cell ratios decreased distinctly in this artificial environment compared to glucose uptake in living organisms. In contrast, we did not observe any significant change in the glucose uptake ratios between astrocytes and non-microglia/non-astrocyte cells after *in vivo* injection or subsequent *in vitro* incubation. These results indicate that microglia, which are known to be highly motile in the brain (Davalos et al., 2005; Nimmerjahn et al., 2005), have reduced energy demand when they do not act in their regular brain environment. This was likely due to the lack of diverse extracellular signals. Chemoattractant triggers such as ADP or ATP (Ohsawa and Kohsaka, 2011; Davalos et al., 2005) or ligands for microglial triggering receptors, such as apolipoproteins for TREM2 (Yeh et al., 2016) regarding pathological activation, are capable of altering microglial activation states (Stence et al., 2001;

Krasemann et al., 2017; Parhizkar et al., 2019). This increases synthesis and transport of neurotransmitters, requiring intermediates in the glycolytic pathway as precursor molecules (Wolosker and Mori, 2012; Dienel, 2019) and induces morphological changes in microglia, resulting in increased cellular motion (Stence et al., 2001), which also consumes glucose for ATP synthesis. In line with our previous study, the elevated [^{18}F]FDG-PET signals observed in mouse models of amyloidosis were mainly driven by activated microglia (Xiang et al., 2021). Hence, supported by our current observations, *in vitro* glucose uptake values should be interpreted with caution because of the reduced cellular energy demand. Furthermore, insulin and insulin-like growth factors (IGF) are recognized as potent modulators of cellular glucose uptake. Indeed, emerging evidence indicates that insulin signaling via IGF substantially regulates microglial metabolism. In this regard, it has been demonstrated that hyperinsulinemia can alter microglial energy metabolism by impairing the membranous expression of GLUT4 (Yang et al., 2022). In addition, brain glucose metabolism was shown to be modulated by insulin, which exerts its effects on astrocytes by interacting with IGF-I (Fernandez et al., 2017). In conjunction with variations in oxygen availability, a lack of these factors *in vitro* may substantially contribute to the observed discrepancies in glucose uptake in the present study when compared to *in vivo*.

Accordingly, our results demonstrated strong differences in the relative [^{18}F]FDG uptake of cultured neurons, astrocytes, and microglia *in vitro* compared to the relative glucose uptake of these cell types in the regular brain environment. Contrary to our *in vivo* results, cultured neurons exhibited by far the highest [^{18}F]FDG uptake (Camandola and Mattson, 2017; Harris et al., 2012), whereas microglia showed the lowest uptake. Although the greater loss of neuronal axons and astrocytic processes during brain dissociation may partially explain this finding, the very low uptake of glucose in microglia relative to that in neurons and astrocytes should still raise awareness to interpret such results with caution. In this regard, recent data from our lab showed a strong impact of astroglial glucose uptake on changes in FDG-PET signals during aging of mice, which cannot be explained by the 82-fold and 8-fold lower glucose uptake by microglia and astrocytes compared to neurons (Bartos et al., 2024a).

In the current study, scRadiotracing was used to provide a snapshot of substrate uptake for energy metabolism (i.e., glucose) at cellular resolution, but the advantages and limitations of this methodology need to be considered. Since the results of this method are expressed as "radioactivity per cell" with normalization to the whole-brain FDG uptake, the loss of cells during the sorting procedure does not critically impact the relative analysis endpoint, regardless of whether they are unequally distributed across cell types. As an internal validation of the head-to-head comparison (*in vivo* vs. *in vitro*), we used an additional setup without *in vivo* injection to demonstrate that *in vivo* [^{18}F]FDG injection prior to *in vitro* incubation did not affect microglial glucose uptake. Moreover, a possible effect of glucose-6-phosphatase activity in brain cells (Broadwell and Cataldo, 1983; Chen et al., 2017; Cossu et al., 2019; Müller et al., 2018), which hydrolyzes FDG-6-phosphate (Welch et al., 2013) and could lead to tracer washout, was reduced to a minimum by the immediate use of a cold buffer due to the enzyme temperature optimum of 37.5 °C (Ababei and Moisiu, 1970; Arcus et al., 2016).

Furthermore, we investigated the influence of strict fasting on cells during scRadiotracing, which may occur after brain dissection and thus arrests hematogenous cellular glucose supply during radioactivity measurements and brain dissociation until the media reassures a comprehensive glucose supply in the single-cell suspension. In this regard, the experiment was repeated equivalently with a glucose-free buffer, whereas the animals were fastened similarly in both setups before the tracer injection. In doing so, microglia and non-microglia/non-astrocyte cells did not show any changes in glucose uptake, either after *in vivo* injection or subsequent *in vitro* incubation. However, strict fasting appeared to affect astrocytes at least slightly by increasing their cellular glucose uptake after *in vivo* injection and *in vitro* incubation, thus suggesting a higher sensitivity to low amounts of glucose. Nevertheless, microglia still showed the highest glucose uptake *in vivo* and *in vitro* in the fasting experiment. This finding may be related to the closely linked metabolism of astrocytes and neurons. Because of the upregulation of glucose uptake and glycolysis, enabled by the protection of toxic byproducts through their glyoxalase system, astrocytes are able to compensate for their ATP demand. Simultaneously, this allows them to support neurons via the astrocyte-neuronal lactate shuttle (ANLS), which substitutes for the neuronal tricarboxylic acid cycle to maintain cellular functions and metabolism (Bélanger et al., 2011; Cleland et al., 2021; Patel et al., 2014). This assumption could be supported by obtaining no significant difference in neuronal [^{18}F]FDG uptake, since neurons have no glyoxalase system compared to astrocytes (Almeida et al., 2004; Bélanger et al., 2011; Herrero-Mendez et al., 2009). However, further studies are required to elucidate the mechanisms underlying this finding.

We also considered the possible cellular saturation effects caused by prior *in vivo* [^{18}F]FDG injection when performing excessive *in vitro* incubation. Our *in vitro* experiment without prior *in vivo* [^{18}F]FDG injection indicated no significant changes in microglia but an increase in astrocytic glucose uptake. However, according to the literature, there is no direct evidence of negative feedback mechanisms that may arise from the phosphorylated product of [^{18}F]FDG. Furthermore, because only astrocytes exhibited changes in *in vitro* glucose uptake values that were associated with varying glucose levels in the buffer used during the workflow, saturation effects caused by [^{18}F]FDG-6-phosphate remain rather unlikely at the concentrations used.

Our approach to cell sorting and glucose uptake measures after *in vivo* tracer injection needs to be interpreted together with established methods of cell metabolism assessment. To understand cellular physiology, several *in vitro* methods, such as the Seahorse assay, allow real-time measurement of cellular metabolism (Caines et al., 2022; Desousa et al., 2023). The Seahorse assay quantifies cellular energy consumption using the oxygen consumption rate (OCR), which is a readout of mitochondrial respiration. Additionally, glycolysis can be monitored by measuring the extracellular acidification rate (ECAR), which reflects acidification of the medium upon lactate secretion (Divakaruni et al., 2014). However, the Seahorse assay acts in a similar *in vitro* environment as our *in vitro* FDG uptake assay. Thus, our head-to-head comparison against *in vivo* glucose uptake indicates that Seahorse results on microglia may be biased by a different metabolic state compared to the experimental conditions in living organisms.

As another method, *ex vivo* metabolomics using mass spectrometry is increasingly applied (Jang et al., 2018) to characterize energy metabolism by measuring the abundance of specific metabolites. However, to use this readout at cell-type resolution,

Kunte et al. 10.3389/fncel.2025.1572431

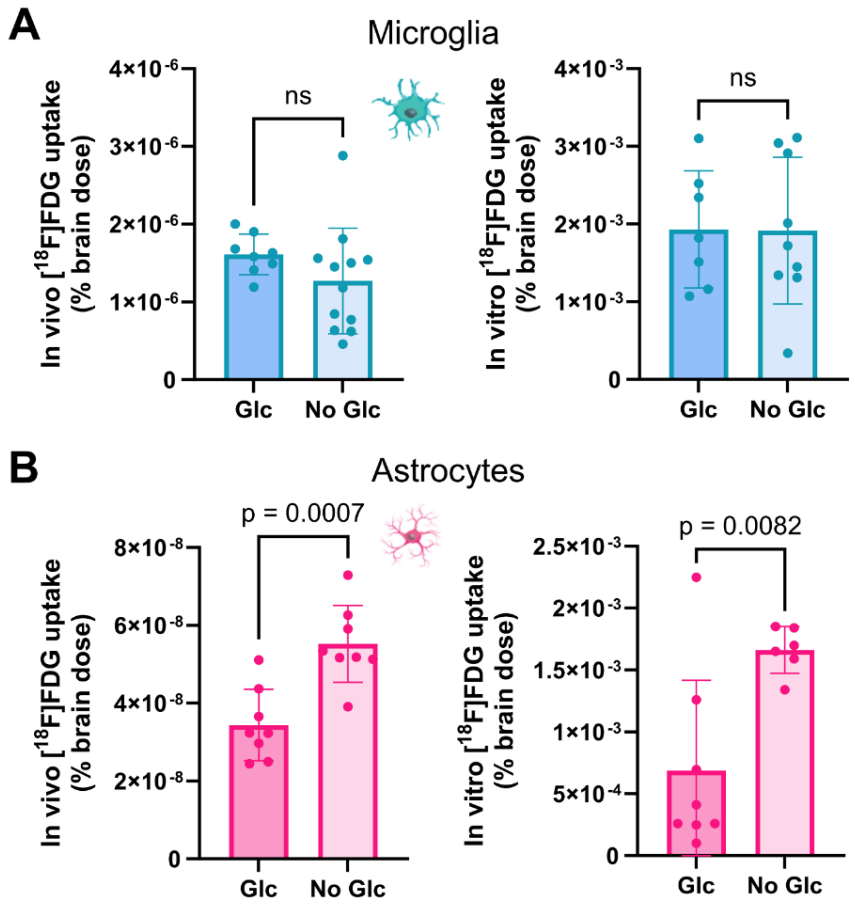

FIGURE 4
Strict fasting increases astrocytic glucose uptake but has no influence on microglial glucose uptake. Comparison of microglial and astrocytic [18F]FDG uptake in a buffer containing glucose and a glucose-free buffer. Fasting had no influence on **(A)** microglial [^{18}F]FDG uptake *in vivo* (top left) or *in vitro* (top right), whereas **(B)** astrocytic [^{18}F]FDG uptake increased significantly *in vivo* (bottom left) or *in vitro* (bottom right).

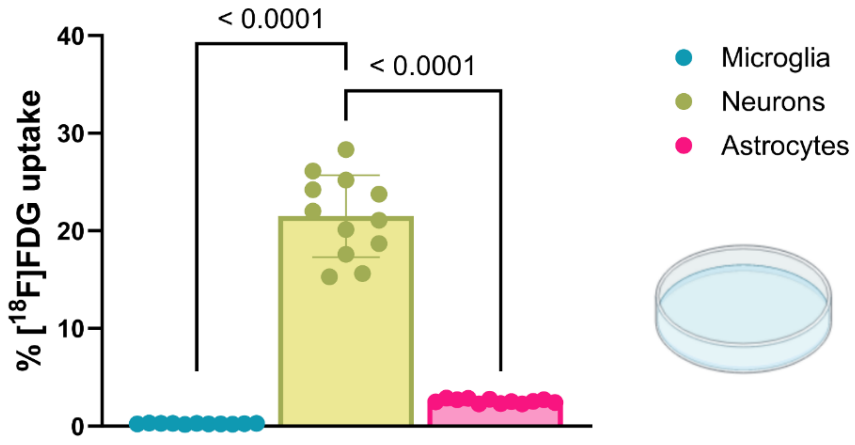

FIGURE 5
Cultured microglia, neurons, and astrocytes display altered glucose uptake compared with cells from a regular brain environment. [^{18}F]FDG *in vitro* incubation showed the highest glucose uptake in cultured neurons, significantly exceeding values observed in cultured microglia and astrocytes.

changes in metabolites during the sorting procedure must be considered, which also accounts for the assessment of glucose transporters and enzymes by transcriptomics (Saliba et al., 2014). Interestingly, it was recently shown that cold 2-DG can be detected by mass spectroscopy (Volland et al., 2022), providing the same snapshot of the trapped glycolysis substrate as in our procedure. The advantage of mass spectroscopy is that it is available at centers without a radioprotective area, whereas scRadiotracing can provide the readout on the day of the experiment.

An important limitation of our approach using scRadiotracing is the loss of axons and processes during brain homogenization. Hence, we assume that by the measurement of cellular bodies solely, glucose uptake values in neurons and astrocytes may be underestimated. In line with this, a hypothetical model showed that only ~30% of FDG uptake in the brains of wild-type mice can be explained by known factors and cellular uptake (Xiang et al., 2022). This finding is especially important for neuronal glucose uptake, since synapses are known as the primary compartment of [^{18}F]FDG uptake (Sokoloff et al., 1977; Sokoloff, 1993, 1999) and may also contribute to significantly different results when comparing scRadiotracing and cell culture data in this study. In line with this issue, we acknowledge that differences in the experimental setups between scRadiotracing and cell culture incubation (i.e., temperature difference, incubation time, and age of cultured cells) may have further amplified the observed changes. However, the potential bias is expected to be of a minor magnitude because these factors are equal to all cell fractions. Furthermore, the calculation of relative cellular uptake ratios likely balanced the impact of setup differences. Our previous study verified the dose dependency of cellular FDG uptake in neurons (Xiang et al., 2021). Hence, it was not possible to directly compare the absolute cellular glucose uptake values after *in vivo* injection with uptake values after excessive *in vitro* [^{18}F]FDG incubation. Therefore, we compared the cellular uptake ratios. [^{18}F]FDG uptake is also influenced by altered cellular activation states, as mentioned above. In this regard, the cell sorting procedure and subsequent cell stress may account for microglial activation, most likely resulting in increased glucose uptake during the *in vitro* incubation. In this regard, *in vitro* incubation at different time points after the sorting procedure should be tested in future investigations to study the impact of cell stress levels on glucose uptake. In addition, cellular-bound [^{18}F]FDG may be released from damaged cells during brain homogenization. However, the entire workflow of scRadiotracing includes multiple dilution and washing steps, which minimize non-cellular bound tracers. Nevertheless, this could contribute to the perceived influence of fasting on astrocytic glucose uptake when a glucose-free buffer is used. Moreover, the microglia/astrocyte-negative cell fraction represents a neuron-enriched fraction with ~80% purity for comparison with the enriched microglia and astrocyte fractions. This may not precisely reflect the observed ratios in contrast to purely isolated neurons. In addition, given that the cellular marker we utilized for the validation of the neuronal proportion is also expressed on T-lymphocytes, it is evident that CD90.2 may not precisely reflect the neuronal proportion. However, since only wild-type mice were included in this study, the supposed impact of very limited amounts of T-lymphocytes on the CD90.2-positive fraction is likely negligible. Additionally, as addressed in a previous study (Bartos et al., 2024a), sex-related disparities in cellular glucose uptake need to be considered. In this regard, one study demonstrated significant alterations in cerebral GLUT expression during the estrus cycle in rats, which may affect the *in vivo* and *in vitro* uptake of glucose depending on the estrus stage (Harrell et al., 2014). Consequently, the restriction of our data to female mice limits the interpretability of the potential sex differences in microglial glucose uptake. In this regard, estrus-related changes in glucose uptake can be pronounced in living organisms, supporting the importance of *in vivo* versus *in vitro* considerations. Ultimately, it needs to be considered that isoflurane used for anesthesia is known to cause dose-dependent hypotension (Gargiulo et al., 2012), and uptake in brain cells is dependent on passing the blood–brain barrier and thus on physiological blood circulation. In this regard, isoflurane could affect relative [^{18}F]FDG uptake by different cell types to a variable extent. Further studies, therefore, need to investigate additional determinants of scRadiotracing to fully understand confounding impacts on cellular glucose uptake.

In conclusion, this study demonstrated that *in vitro* measurements of microglial energy metabolism might be misleading because of the lack of influence of the *in vivo* environment. Astrocytes appear to have a higher sensitivity to low glucose levels than microglia do. For the investigation of cellular energy metabolism, there are several methods providing *in vivo* and *ex vivo* applicability. scRadiotracing facilitates substantial assessment of *in vivo* glucose metabolism, allows simple combination with other methods for extended workflows, and provides insufficient cellular resolution.

Data availability statement

The original contributions presented in the study are included in the article/supplementary material, further inquiries can be directed to the corresponding author/s.

Ethics statement

The animal study was approved by Regierung von Oberbayern, Munich, Germany. The study was conducted in accordance with the local legislation and institutional requirements.

Author contributions

SK: Writing – original draft, Writing – review & editing. JG: Writing – review & editing. PB: Writing – review & editing. LB: Writing – review & editing. SW: Writing – review & editing. KW-M: Writing – review & editing. AH: Writing – review & editing. DP: Writing – review & editing. RW: Writing – review & editing. SZ: Writing – review & editing. NA: Writing – review & editing. AC: Writing – review & editing. ST: Writing – review & editing. MB: Writing – original draft, Writing – review & editing.

Funding

The author(s) declare that financial support was received for the research and/or publication of this article. JG was funded by the Munich Clinician Scientist Program (MCSP). AH was funded by the

Deutsche Forschungsgemeinschaft (DFG, German Research Foundation—ID 545058105). MB was funded by the Deutsche Forschungsgemeinschaft (DFG) under Germany's Excellence Strategy within the framework of the Munich Cluster for Systems Neurology (EXC 2145 SyNergy—ID 390857198).

Conflict of interest

MB is a member of the Neuroimaging Committee of the EANM. MB has received speaker honoraria from Roche, GE Healthcare, Iba, and Life Molecular Imaging; has advised Life Molecular Imaging and GE Healthcare; and is currently on the advisory board of MIAC. AH reports compensation for scientific consulting by ABX advanced biochemical compounds outside the submitted work.

The remaining authors declare that the research was conducted in the absence of any commercial or financial relationships that could be construed as a potential conflict of interest.

Generative AI statement

The authors declare that no Gen AI was used in the creation of this manuscript.

Any alternative text (alt text) provided alongside figures in this article has been generated by Frontiers with the support of artificial intelligence and reasonable efforts have been made to ensure accuracy, including review by the authors wherever possible. If you identify any issues, please contact us.

Publisher's note

All claims expressed in this article are solely those of the authors and do not necessarily represent those of their affiliated organizations, or those of the publisher, the editors and the reviewers. Any product that may be evaluated in this article, or claim that may be made by its manufacturer, is not guaranteed or endorsed by the publisher.

References

Ababei, L., and Moisiu, M. (1970). On the activity of glucose-6-phosphate phosphohydrolase in the red blood cells. *Blut* 20, 363–369. doi: 10.1007/BF01634046

Almeida, A., Moncada, S., and Bolaños, J. P. (2004). Nitric oxide switches on glycolysis through the AMP protein kinase and 6-phosphofructo-2-kinase pathway. *Nat. Cell Biol.* 6, 45–51. doi: 10.1038/ncb1080

Arcus, V. L., Prentice, E. J., Hobbs, J. K., Mulholland, A. J., Van der Kamp, M. W., Pudney, C. R., et al. (2016). On the temperature dependence of enzyme-catalyzed rates. *Biochemistry* 55, 1681–1688. doi: 10.1021/acs.biochem.5b01094

Bartos, L. M., Kirchleitner, S. V., Kolabas, Z. I., Quach, S., Beck, A., Lorenz, J., et al. (2023). Deciphering sources of PET signals in the tumor microenvironment of glioblastoma at cellular resolution. *Sci. Adv.* 9:eadi8986. doi: 10.1126/sciadv.adi8986

Bartos, L. M., Kunte, S. T., Beumers, P., Xiang, X., Wind, K., Ziegler, S., et al. (2022). Single cell radiotracer allocation via immunomagentic sorting (scRadiotracing) to disentangle PET signals at cellular resolution. *J. Nucl. Med.* 63, 1459–1462. doi: 10.2967/jnumed.122.264171

Bartos, L. M., Kunte, S. T., Wagner, S., Beumers, P., Schaefer, R., Zatcepin, A., et al. (2024a). Astroglial glucose uptake determines brain FDG-PET alterations and metabolic connectivity during healthy aging in mice. *NeuroImage* 300:120860. doi: 10.1016/j.neuroimage.2024.120860

Bartos, L. M., Quach, S., Zenatti, V., Kirchleitner, S. V., Blobner, J., Wind-Mark, K., et al. (2024b). Remote Neuroinflammation in newly diagnosed glioblastoma correlates with unfavorable clinical outcome. *Clin. Cancer Res.* 30, 4618–4634. doi: 10.1158/1078-0432.CCR-24-1563

Bélanger, M., Yang, J., Petit, J. M., Laroche, T., Magistretti, P. J., and Allaman, I. (2011). Role of the glyoxalase system in astrocyte-mediated neuroprotection. *J. Neurosci.* 31, 18338–18352. doi: 10.1523/JNEUROSCI.1249-11.2011

Bernier, L. P., York, E. M., Kamyabi, A., Choi, H. B., Weilinger, N. L., and MacVicar, B. A. (2020). Microglial metabolic flexibility supports immune surveillance of the brain parenchyma. *Nat. Commun.* 11:1559. doi: 10.1038/s41467-020-15267-z

Broadwell, R. D., and Cataldo, A. M. (1983). The neuronal endoplasmic reticulum: its cytochemistry and contribution to the endomembrane system. I. Cell bodies and dendrites. *J. Histochem. Cytochem.* 31, 1077–1088. doi: 10.1177/31.9.6309951

Bubber, P., Haroutunian, V., Fisch, G., Blass, J. P., and Gibson, G. E. (2005). Mitochondrial abnormalities in Alzheimer brain: mechanistic implications. *Ann. Neurol.* 57, 695–703. doi: 10.1002/ana.20474

Caines, J. K., Barnes, D. A., and Berry, M. D. (2022). The use of seahorse XF assays to interrogate real-time energy metabolism in Cancer cell lines. *Methods Mol. Biol.* 2508, 225–234. doi: 10.1007/978-1-0716-2376-3_17

Camandola, S., and Mattson, M. P. (2017). Brain metabolism in health, aging, and neurodegeneration. *EMBO J.* 36, 1474–1492. doi: 10.15252/embj.201695810

Chen, J., Wang, T., Zhou, X. Y., Tang, C. X., and Gao, D. S. (2017). Glucose-6-phosphatase-α participates in dopaminergic differentiation. *Neurol. Res.* 39, 869–876. doi: 10.1080/01616412.2017.1348681

Choi, H., Choi, Y., Lee, E. J., Kim, H., Lee, Y., Kwon, S., et al. (2021). Hippocampal glucose uptake as a surrogate of metabolic change of microglia in Alzheimer's disease. *J. Neuroinflammation* 18:190. doi: 10.1186/s12974-021-02244-6

Cleland, N. R. W., Al-Juboori, S. I., Dobrinskikh, E., and Bruce, K. D. (2021). Altered substrate metabolism in neurodegenerative disease: new insights from metabolic imaging. *J. Neuroinflammation* 18:248. doi: 10.1186/s12974-021-02305-w

Cossu, V., Marini, C., Piccioli, P., Rocchi, A., Bruno, S., Orengo, A. M., et al. (2019). Obligatory role of endoplasmic reticulum in brain FDG uptake. *Eur. J. Nucl. Med. Mol. Imaging* 46, 1184–1196. doi: 10.1007/s00259-018-4254-2

Davalos, D., Grutzendler, J., Yang, G., Kim, J. V., Zuo, Y., Jung, S., et al. (2005). ATP mediates rapid microglial response to local brain injury in vivo. *Nat. Neurosci.* 8, 752–758. doi: 10.1038/nn1472

Desousa, B. R., Kim, K. K., Jones, A. E., Ball, A. B., Hsieh, W. Y., Swain, P., et al. (2023). Calculation of ATP production rates using the seahorse XF analyzer. *EMBO Rep.* 24:e56380. doi: 10.15252/embr.202256380

Dienel, G. A. (2019). Brain glucose metabolism: integration of energetics with function. *Physiol. Rev.* 99, 949–1045. doi: 10.1152/physrev.00062.2017

Dinkel, L., Hummel, S., Zenatti, V., Malara, M., Tillmann, Y., Colombo, A., et al. (2024). Myeloid cell-specific loss of NPC1 in mice recapitulates microgliosis and neurodegeneration in patients with Niemann-pick type C disease. *Sci. Transl. Med.* 16:eadl4616. doi: 10.1126/scitranslmed.adl4616

Divakaruni, A. S., Paradyse, A., Ferrick, D. A., Murphy, A. N., and Jastroch, M. (2014). Analysis and interpretation of microplate-based oxygen consumption and pH data. *Methods Enzymol.* 547, 309–354. doi: 10.1016/B978-0-12-801415-8.00016-3

Fernandez, A. M., Hernandez-Garzón, E., Perez-Domper, P., Perez-Alvarez, A., Mederos, S., Matsui, T., et al. (2017). Insulin regulates astrocytic glucose handling through cooperation with IGF-I. *Diabetes* 66, 64–74. doi: 10.2337/db16-0861

Fumagalli, M., Lombardi, M., Gressens, P., and Verderio, C. (2018). How to reprogram microglia toward beneficial functions. *Glia* 66, 2531–2549. doi: 10.1002/glia.23484

Gao, T., Xiao, H., Ramesha, S., Seyfried, N. T., Levey, A. I., and Rangaraju, S. (2019). O4-09-02: regulation of pro-inflammatory and disease-associated microglial activation by BIN1. *Alzheimers Dement.* 15:P1256.

Gargiulo, S., Greco, A., Gramanzini, M., Esposito, S., Affuso, A., Brunetti, A., et al. (2012). Mice anesthesia, analgesia, and care, Part I: anesthetic considerations in preclinical research. *Ilar J.* 53, E55–E69. doi: 10.1093/ilar.53.1.55

Gnörich, J., Reifschneider, A., Wind, K., Zatcepin, A., Kunte, S. T., Beumers, P., et al. (2023). Depletion and activation of microglia impact metabolic connectivity of the mouse brain. *J. Neuroinflammation* 20:47. doi: 10.1186/s12974-023-02735-8

Hammond, T. R., Dufort, C., Dissing-Olesen, L., Giera, S., Young, A., Wysoker, A., et al. (2019). Single-cell RNA sequencing of microglia throughout the mouse lifespan and in the injured brain reveals complex cell-state changes. *Immunity* 50, 253–71.e6. doi: 10.1016/j.immuni.2018.11.004

Harrell, C. S., Burgado, J., Kelly, S. D., and Neigh, G. N. (2014). Ovarian steroids influence cerebral glucose transporter expression in a region- and isoform-specific pattern. *J. Neuroendocrinol.* 26, 217–225. doi: 10.1111/jne.12139

Harris, J. J., Jolivet, R., and Attwell, D. (2012). Synaptic energy use and supply. *Neuron* 75, 762–777. doi: 10.1016/j.neuron.2012.08.019

Herrero-Mendez, A., Almeida, A., Fernández, E., Maestre, C., Moncada, S., and Bolaños, J. P. (2009). The bioenergetic and antioxidant status of neurons is controlled by continuous degradation of a key glycolytic enzyme by APC/C-Cdh1. *Nat. Cell Biol.* 11, 747–752. doi: 10.1038/ncb1881

Hrovatin, K., Fischer, D. S., and Theis, F. J. (2022). Toward modeling metabolic state from single-cell transcriptomics. *Mol Metab* 57:101396. doi: 10.1016/j.molmet.2021.101396

Jang, C., Chen, L., and Rabinowitz, J. D. (2018). Metabolomics and isotope tracing. *Cell* 173, 822–837. doi: 10.1016/j.cell.2018.03.055

Jung, E. S., Choi, H., and Mook-Jung, I. (2025). Decoding microglial immunometabolism: a new frontier in Alzheimer's disease research. *Mol. Neurodegener.* 20:37. doi: 10.1186/s13024-025-00825-0

Kaech, S., and Banker, G. (2006). Culturing hippocampal neurons. *Nat. Protoc.* 1, 2406–2415. doi: 10.1038/nprot.2006.356

Krasemann, S., Madore, C., Cialic, R., Baufeld, C., Calcagno, N., El Fatimy, R., et al. (2017). The TREM2-APOE pathway drives the transcriptional phenotype of dysfunctional microglia in neurodegenerative diseases. *Immunity* 47, 566–81.e9. doi: 10.1016/j.immuni.2017.08.008

Mattson, M. P. (2004). Pathways towards and away from Alzheimer's disease. *Nature* 430, 631–639. doi: 10.1038/nature02621

Minoshima, S., Cross, D., Thientunyakit, T., Foster, N. L., and Drzezga, A. (2022). (18) F-FDG PET imaging in neurodegenerative dementing disorders: insights into subtype classification, emerging disease categories, and mixed dementia with copathologies. *J. Nucl. Med.* 63, 2s–12s. doi: 10.2967/jnumed.121.263194

Montagna, E., Crux, S., Luckner, M., Herber, J., Colombo, A. V., Marinković, P., et al. (2019). In vivo ca(2+) imaging of astrocytic microdomains reveals a critical role of the amyloid precursor protein for mitochondria. *Glia* 67, 985–998. doi: 10.1002/glia.23584

Moreira, P. I., Santos, M. S., Seiça, R., and Oliveira, C. R. (2007). Brain mitochondrial dysfunction as a link between Alzheimer's disease and diabetes. *J. Neurol. Sci.* 257, 206–214. doi: 10.1016/j.jns.2007.01.017

Mosconi, L. (2005). Brain glucose metabolism in the early and specific diagnosis of alzheimer?S disease. *EJNMMI Rep* 32, 486–510. doi: 10.1007/s00259-005-1762-7

Müller, M. S., Fouyssac, M., and Taylor, C. W. (2018). Effective glucose uptake by human astrocytes requires its sequestration in the endoplasmic reticulum by Glucose-6-phosphatase-β. *Curr. Biol.* 28, 3481–86.e4. doi: 10.1016/j.cub.2018.08.060

Nimmerjahn, A., Kirchhoff, F., and Helmchen, F. (2005). Resting microglial cells are highly dynamic surveillants of brain parenchyma in vivo. *Science* 308, 1314–1318. doi: 10.1126/science.1110647

Ohsawa, K., and Kohsaka, S. (2011). Dynamic motility of microglia: purinergic modulation of microglial movement in the normal and pathological brain. *Glia* 59, 1793–1799. doi: 10.1002/glia.21238

Olah, M., Menon, V., Habib, N., Taga, M. F., Ma, Y., Yung, C. J., et al. (2020). Single cell RNA sequencing of human microglia uncovers a subset associated with Alzheimer's disease. *Nat. Commun.* 11:6129. doi: 10.1038/s41467-020-19737-2

Orihuela, R., McPherson, C. A., and Harry, G. J. (2016). Microglial M1/M2 polarization and metabolic states. *Br. J. Pharmacol.* 173, 649–665. doi: 10.1111/bph.13139

Parhizkar, S., Arzberger, T., Brendel, M., Kleinberger, G., Deussing, M., Focke, C., et al. (2019). Loss of TREM2 function increases amyloid seeding but reduces plaque-associated ApoE. *Nat. Neurosci.* 22, 191–204. doi: 10.1038/s41593-018-0296-9

Patel, A. B., Lai, J. C., Chowdhury, G. M., Hyder, F., Rothman, D. L., Shulman, R. G., et al. (2014). Direct evidence for activity-dependent glucose phosphorylation in neurons with implications for the astrocyte-to-neuron lactate shuttle. *Proc. Natl. Acad. Sci. USA* 111, 5385–5390. doi: 10.1073/pnas.1403576111

Rauchmann, B. S., Brendel, M., Franzmeier, N., Trappmann, L., Zaganjori, M., Ersoezlue, E., et al. (2022). Microglial activation and connectivity in Alzheimer disease and aging. *Ann. Neurol.* 92, 768–781. doi: 10.1002/ana.26465

Saliba, A. E., Westermann, A. J., Gorski, S. A., and Vogel, J. (2014). Single-cell RNA-seq: advances and future challenges. *Nucleic Acids Res.* 42, 8845–8860. doi: 10.1093/nar/gku555

Slemann, L., Gnörich, J., Hummel, S., Bartos, L. M., Klaus, C., Kling, A., et al. (2024). Neuronal and oligodendroglial, but not astroglial, tau translates to in vivo tau PET signals in individuals with primary tauopathies. *Acta Neuropathol.* 148:70. doi: 10.1007/s00401-024-02834-7

Sokoloff, L. (1993). Sites and mechanisms of function-related changes in energy metabolism in the nervous system. *Dev. Neurosci.* 15, 194–206. doi: 10.1159/000111335

Sokoloff, L. (1999). Energetics of functional activation in neural tissues. *Neurochem. Res.* 24, 321–329. doi: 10.1023/A:1022534709672

Sokoloff, L., Reivich, M., Kennedy, C., Des Rosiers, M. H., Patlak, C. S., Pettigrew, K. D., et al. (1977). The [14C]deoxyglucose method for the measurement of local cerebral glucose utilization: theory, procedure, and normal values in the conscious and anesthetized albino rat. *J. Neurochem.* 28, 897–916. doi: 10.1111/j.1471-4159.1977.tb10649.x

Stence, N., Waite, M., and Dailey, M. E. (2001). Dynamics of microglial activation: a confocal time-lapse analysis in hippocampal slices. *Glia* 33, 256–266. doi: 10.1002/1098-1136(200103)33:3<256::AID-GLIA1024>3.0.CO;2-J

Ueda, T. (2016). Vesicular Glutamate Uptake. *Adv Neurobiol* 13, 173–221. doi: 10.1007/978-3-319-45096-4_7

Volland, J. M., Kaupp, J., Schmitz, W., Wünsch, A. C., Balint, J., Möllmann, M., et al. (2022). Mass spectrometric metabolic fingerprinting of 2-deoxy-D-glucose (2-DG)-induced inhibition of glycolysis and comparative analysis of methionine restriction versus glucose restriction under perfusion culture in the murine L929 model system. *Int. J. Mol. Sci.* 23:9220. doi: 10.3390/ijms23169220

Wallace, D. C. (2005). A mitochondrial paradigm of metabolic and degenerative diseases, aging, and cancer: a dawn for evolutionary medicine. *Annu. Rev. Genet.* 39, 359–407. doi: 10.1146/annurev.genet.39.110304.095751

Welch, A., Mingarelli, M., Riedel, G., and Platt, B. (2013). Mapping changes in mouse brain metabolism with PET/CT. *J. Nucl. Med.* 54, 1946–1953. doi: 10.2967/jnumed.113.121509

Willem, M., Tahirovic, S., Busche, M. A., Ovsepian, S. V., Chafai, M., Kootar, S., et al. (2015). η-Secretase processing of APP inhibits neuronal activity in the hippocampus. *Nature* 526, 443–447. doi: 10.1038/nature14864

Wolosker, H., and Mori, H. (2012). Serine racemase: an unconventional enzyme for an unconventional transmitter. *Amino Acids* 43, 1895–1904. doi: 10.1007/s00726-012-1370-3

Xiang, X., Tahirovic, S., Ziegler, S., Haass, C., and Brendel, M. (2022). Response to comment on "microglial activation states drive glucose uptake and FDG-PET alterations in neurodegenerative diseases". *Sci. Transl. Med.* 14:eabn5104. doi: 10.1126/scitranslmed.abn5104

Xiang, X., Wind, K., Wiedemann, T., Blume, T., Shi, Y., Briel, N., et al. (2021). Microglial activation states drive glucose uptake and FDG-PET alterations in neurodegenerative diseases. *Sci. Transl. Med.* 13:eabe5640. doi: 10.1126/scitranslmed.abe5640

Yang, X., Xu, Y., Gao, W., Wang, L., Zhao, X., Liu, G., et al. (2022). Hyperinsulinemia-induced microglial mitochondrial dynamic and metabolic alterations lead to neuroinflammation in vivo and in vitro. *Front. Neurosci.* 16:1036872. doi: 10.3389/fnins.2022.1036872

Yeh, F. L., Wang, Y., Tom, I., Gonzalez, L. C., and Sheng, M. (2016). TREM2 binds to apolipoproteins, including APOE and CLU/APOJ, and thereby facilitates uptake of amyloid-Beta by microglia. *Neuron* 91, 328–340. doi: 10.1016/j.neuron.2016.06.015

Zhang, Y., Chen, K., Sloan, S. A., Bennett, M. L., Scholze, A. R., O'Keeffe, S., et al. (2014). An RNA-sequencing transcriptome and splicing database of glia, neurons, and vascular cells of the cerebral cortex. *J. Neurosci.* 34, 11929–11947. doi: 10.1523/JNEUROSCI.1860-14.2014

Zhang, X., Yuan, T., Keijer, J., and de Boer, V. C. J. (2021). OCRbayes: a Bayesian hierarchical modeling framework for seahorse extracellular flux oxygen consumption rate data analysis. *PLoS One* 16:e0253926. doi: 10.1371/journal.pone.0253926

5. Ausblick

Die Ergebnisse der zugrundeliegenden Publikation dieser Dissertationsschrift zeigen, dass sich scRadiotracing zukünftig zu einem wertvollen Hilfsmittel in der Erforschung neurodegenerativer Erkrankungen etablieren könnte. Zum Verständnis der zellulären und molekularen, physiologischen wie pathologischen Veränderungen bietet die Untersuchung des mikroglialen Energiestoffwechsels eine wesentliche Grundlage. Mit zunehmendem Wissen über mikrogliale Schlüsselfunktionen und metabolische Interaktionen zwischen Hirnzellen, könnten sich zudem weitere Ansätze zur Therapie neurodegenerativer Erkrankungen wie Morbus Alzheimer erschließen.

Mit der im großen Kontext assoziierter Projekte etablierten und weiterentwickelten Methodik des scRadiotracing, wurden im Rahmen dieser Dissertation die Relevanz der *in vivo* Erforschung des mikroglialen Metabolismus aufgezeigt. Vorteile des neuartigen Workflows konnten durch Implementierung in der präklinischen nuklearmedizinischen Forschung näher beleuchtet werden.

In diesem Zusammenhang wurde durch Kombination von PET/CT-Bildgebung mit funktionelle MRT (fMRT) und scRadiotracing, als bisher unbekannte zelluläre Quelle der metabolischen Konnektivität im Gehirn, die maßgebliche mikrogliale ^{18}F-FDG-Aufnahme identifiziert [38]. In einer Folgestudie wurde basierend auf diesen Erkenntnissen, durch ein ganzheitliches Konzept aus PET-Bildgebung und scRadiotracing, die astrozytäre und mikrogliale Glukoseaufnahme als wesentliche Einflussfaktoren der metabolischen Konnektivität und des zunehmenden zerebralen Glukosestoffwechsels mit fortschreitendem Alter identifiziert [41]. Weitere Studien werden die metabolische Synergie zwischen Mikroglia und den anderen Hirnzellen detaillierter untersuchen müssen. Ungeklärt bleibt weiterhin, ob Mikroglia alleine für ihren hohen Glukoseverbrauch verantwortlich sind oder ob die Energieaufnahme in anderen Zellen stattfindet und durch Mechanismen wie ein fragliches Mikroglia-Neuron-Shuttle verteilt wird.

scRadiotracing kann, neben der Untersuchung des zellulären Glukosemetabolismus mit ^{18}F-FDG als Radiotracer, vielfältig eingesetzt werden. Die flexible Anpassung des Workflows zur Isolation von Zellpopulationen und der Einsatz diverser Radiotracer bietet die Möglichkeit der Untersuchung pathophysiologisch differenter

neurodegenerativer Erkrankungen [42, 43] sowie zerebraler Tumorerkrankungen und assoziierter Neuroinflammation [21, 37, 39, 40].

Die Methodik des scRadiotracing weist derzeit allerdings noch Limitationen auf. Unter anderem ist es noch nicht möglich den Verlust an Zellfortsätzen während der mechanischen Probenaufbereitung zu bestimmen, was zu potenzieller Fehleinschätzung der zellulären Tracerzuordnung führen kann. Bei Verwendung von ^{18}F-FDG betrifft dies insbesondere Neuronen, bei denen die Literatur vermutet, dass sich ein großer Anteil des Tracers in den Synapsen befindet [16, 69, 70]. Um dies näher zu evaluieren werden weitere Studien notwendig sein, auch um den Verlust von ^{18}F-FDG, bei Absterben der Zellen während des Versuchs, über beschädigte Zellmembranen auszuschließen. Nachdem im Rahmen dieser Promotionsarbeit bereits ein Effekt der *in vivo* Tracerinjektion und der zellulären Nüchternheit auf die Ergebnisse ausgeschlossen wurde, müssen zukünftig weitere Determinanten des scRadiotracing untersucht werden.

Insgesamt präsentiert die Kombination von scRadiotracing mit weiteren Methoden wie PET [72] oder Autoradiographie [16] sowie weiteren molekularbiologischen Methoden vielfältige Einsatzmöglichkeiten. Die weitere Entwicklung dieses Verfahrens verfolgt unter anderem das Ziel einer Anwendung in der klinischen Diagnostik. Aufgrund des umfangreichen Workflows begrenzen sich diese allerdings auf die Grundlagenforschung und verhindern derzeit noch einen Einsatz in der klinischen Routine [21].

Mit Bezug auf gegenwärtige Forschungsschwerpunkte der neurologischen Kleintiermedizin könnte die Kombination der beschriebenen Methoden als multimodaler Ansatz neue Erkenntnisse liefern.
Die kanine idiopathische Epilepsie stellt in diesem Zusammenhang einen vielversprechenden Kandidaten dar – eine Erkrankung, für die bis heute keine zugrundeliegende Ätiologie identifiziert werden konnte und die lediglich eine Ausschlussdiagnose darstellt. Eine kurative Behandlung dieser ist demnach nicht möglich und die lebenslange, mit schweren Nebenwirkungen behaftete Therapie stellt für Patienten und Tierbesitzer eine immense Belastung dar [73-76]. Der komplementäre Einsatz von ^{18}F-FDG-PET/CT könnte die im Rahmen der diagnostischen Aufarbeitung durchgeführte MRT um wertvolle Einblicke in die zerebrale Stoffwechsellage und mikrostrukturelle Läsionen ergänzen [77, 78].

Darüber hinaus könnte der diagnostische Einsatz von PET/CT die Diagnostik und Prognostik von Tumorerkrankungen fundamental verbessern. Die klinische Signifikanz dieser Bildgebungstechnik in der Humanmedizin ist bereits bewiesen, insofern, als das therapeutische Management bei bis zu 50% der Patienten beeinflusst wurde [79]. Mögliche Ziele hierbei sind die Quantifizierung und Charakterisierung des therapeutischen Targets mitsamt assoziierter Tumormikroumgebung [37] für eine präzise chirurgische Resektion sowie die Einschätzung eines Therapieerfolges [80].
Für die Evaluation dieser Einsatzmöglichkeiten liefern bereits generierte oder biopsie-basierte scRadiotracing-Daten die Basis zur Interpretation der Ergebnisse auf zellulärer Ebene [39].

Des Weiteren könnte dieser Ansatz zu einer signifikanten Reduktion präklinischer Tierversuche durch den Einsatz natürlich erkrankter Individuen als Tiermodelle beitragen. Die minimal-invasive Untersuchung am lebenden Patienten erlaubt longitudinale Studien ohne den zusätzlichen Bedarf an Versuchstierkohorten. Langfristig geplante Projekte könnten derartige klinische Parameter um postmortale neuropathologische und molekularbiologische Analysen komplementieren. Die translationale Relevanz derartiger Studien für die Humanmedizin muss noch genauer evaluiert werden.

Gegenwärtig ist der Einsatz von PET/CT-Bildgebung in der Tiermedizin jedoch aufgrund eingeschränkter Verfügbarkeit von Radiotracern und Infrastruktur sowie strahlungsbedingter Maßnahmen für den Personenschutz limitiert [81]. Gleichwohl stellen die simultane Grundlagenforschung und gewinnbringende diagnostische Erkenntnisse eine vielversprechende Perspektive dar. Die Zusammenarbeit mit humanmedizinischen Einrichtungen ist daher von größter Signifikanz für die Implementierung dieser Bildgebungsmethodik in die tiermedizinische Diagnostik und Forschung.

6. Literaturverzeichnis

1. Bubber, P., et al., *Mitochondrial abnormalities in Alzheimer brain: mechanistic implications.* Ann Neurol, 2005. **57**(5): p. 695-703.
2. Liang, W.S., et al., *Alzheimer's disease is associated with reduced expression of energy metabolism genes in posterior cingulate neurons.* Proc Natl Acad Sci U S A, 2008. **105**(11): p. 4441-6.
3. Lin, M.T. and M.F. Beal, *Mitochondrial dysfunction and oxidative stress in neurodegenerative diseases.* Nature, 2006. **443**(7113): p. 787-95.
4. Mattson, M.P., *Pathways towards and away from Alzheimer's disease.* Nature, 2004. **430**(7000): p. 631-9.
5. Moreira, P.I., et al., *Brain mitochondrial dysfunction as a link between Alzheimer's disease and diabetes.* J Neurol Sci, 2007. **257**(1-2): p. 206-14.
6. Wallace, D.C., *A mitochondrial paradigm of metabolic and degenerative diseases, aging, and cancer: a dawn for evolutionary medicine.* Annu Rev Genet, 2005. **39**: p. 359-407.
7. Gouras, G.K., T.T. Olsson, and O. Hansson, *β-Amyloid peptides and amyloid plaques in Alzheimer's disease.* Neurotherapeutics, 2015. **12**(1): p. 3-11.
8. Haass, C. and D.J. Selkoe, *Soluble protein oligomers in neurodegeneration: lessons from the Alzheimer's amyloid β-peptide.* Nature Reviews Molecular Cell Biology, 2007. **8**(2): p. 101-112.
9. Näslund, J., et al., *Correlation between elevated levels of amyloid beta-peptide in the brain and cognitive decline.* Jama, 2000. **283**(12): p. 1571-7.
10. Wang, J., et al., *The levels of soluble versus insoluble brain Abeta distinguish Alzheimer's disease from normal and pathologic aging.* Exp Neurol, 1999. **158**(2): p. 328-37.
11. Yankner, B.A., L.K. Duffy, and D.A. Kirschner, *Neurotrophic and neurotoxic effects of amyloid beta protein: reversal by tachykinin neuropeptides.* Science, 1990. **250**(4978): p. 279-82.
12. Baumgartner, A., et al., *Cerebral FDG-PET and MRI findings in autoimmune limbic encephalitis: correlation with autoantibody types.* J Neurol, 2013. **260**(11): p. 2744-53.
13. Guedj, E., et al., *EANM procedure guidelines for brain PET imaging using [(18)F]FDG, version 3.* Eur J Nucl Med Mol Imaging, 2022. **49**(2): p. 632-651.
14. Jack, C.R., Jr., et al., *NIA-AA Research Framework: Toward a biological definition of Alzheimer's disease.* Alzheimers Dement, 2018. **14**(4): p. 535-562.
15. Nelson, T., et al., *Reexamination of Glucose-6-Phosphatase Activity in the Brain in Vivo: No Evidence for a Futile Cycle.* Science, 1985. **229**(4708): p. 60-62.
16. Sokoloff, L., et al., *The [14C]deoxyglucose method for the measurement of local cerebral glucose utilization: theory, procedure, and normal values in the conscious and anesthetized albino rat.* J Neurochem, 1977. **28**(5): p. 897-916.
17. Dave, A., et al., *FDG-PET Imaging of Dementia and Neurodegenerative Disease.* Seminars in Ultrasound, CT and MRI, 2020. **41**(6): p. 562-571.
18. Minoshima, S., et al., *¹⁸F-FDG PET Imaging in Neurodegenerative Dementing Disorders: Insights into Subtype Classification, Emerging Disease Categories, and Mixed Dementia with Copathologies.* Journal of Nuclear Medicine, 2022. **63**(Supplement 1): p. 2S-12S.

19. Choi, H., et al., *Hippocampal glucose uptake as a surrogate of metabolic change of microglia in Alzheimer's disease.* J Neuroinflammation, 2021. **18**(1): p. 190.
20. Xiang, X., et al., *Microglial activation states drive glucose uptake and FDG-PET alterations in neurodegenerative diseases.* Science Translational Medicine, 2021. **13**(615): p. eabe5640.
21. Bartos, L.M., et al., *Single cell radiotracer allocation via immunomagentic sorting (scRadiotracing) to disentangle PET signals at cellular resolution.* J Nucl Med, 2022.
22. Ulland, T.K., et al., *TREM2 Maintains Microglial Metabolic Fitness in Alzheimer's Disease.* Cell, 2017. **170**(4): p. 649-663.e13.
23. Zimmer, E.R., et al., *[(18)F]FDG PET signal is driven by astroglial glutamate transport.* Nat Neurosci, 2017. **20**(3): p. 393-395.
24. Al Samri, M.T., et al., *Measurement of oxygen consumption by murine tissues in vitro.* J Pharmacol Toxicol Methods, 2011. **63**(2): p. 196-204.
25. Lo, L.W., C.J. Koch, and D.F. Wilson, *Calibration of oxygen-dependent quenching of the phosphorescence of Pd-meso-tetra (4-carboxyphenyl) porphine: a phosphor with general application for measuring oxygen concentration in biological systems.* Anal Biochem, 1996. **236**(1): p. 153-60.
26. Lu, H., et al., *Comparative evaluation of software for deconvolution of metabolomics data based on GC-TOF-MS.* TrAC Trends in Analytical Chemistry, 2008. **27**(3): p. 215-227.
27. Jang, C., L. Chen, and J.D. Rabinowitz, *Metabolomics and Isotope Tracing.* Cell, 2018. **173**(4): p. 822-837.
28. Davalos, D., et al., *ATP mediates rapid microglial response to local brain injury in vivo.* Nat Neurosci, 2005. **8**(6): p. 752-8.
29. Ohsawa, K. and S. Kohsaka, *Dynamic motility of microglia: purinergic modulation of microglial movement in the normal and pathological brain.* Glia, 2011. **59**(12): p. 1793-9.
30. Yeh, F.L., et al., *TREM2 Binds to Apolipoproteins, Including APOE and CLU/APOJ, and Thereby Facilitates Uptake of Amyloid-Beta by Microglia.* Neuron, 2016. **91**(2): p. 328-40.
31. Krasemann, S., et al., *The TREM2-APOE Pathway Drives the Transcriptional Phenotype of Dysfunctional Microglia in Neurodegenerative Diseases.* Immunity, 2017. **47**(3): p. 566-581.e9.
32. Parhizkar, S., et al., *Loss of TREM2 function increases amyloid seeding but reduces plaque-associated ApoE.* Nat Neurosci, 2019. **22**(2): p. 191-204.
33. Stence, N., M. Waite, and M.E. Dailey, *Dynamics of microglial activation: a confocal time-lapse analysis in hippocampal slices.* Glia, 2001. **33**(3): p. 256-66.
34. Ueda, T., *Vesicular Glutamate Uptake.* Adv Neurobiol, 2016. **13**: p. 173-221.
35. Wolosker, H. and H. Mori, *Serine racemase: an unconventional enzyme for an unconventional transmitter.* Amino Acids, 2012. **43**(5): p. 1895-904.
36. Dienel, G.A., *Brain Glucose Metabolism: Integration of Energetics with Function.* Physiol Rev, 2019. **99**(1): p. 949-1045.
37. Bartos, L.M., et al., *Deciphering sources of PET signals in the tumor microenvironment of glioblastoma at cellular resolution.* Sci Adv, 2023. **9**(43): p. eadi8986.
38. Gnörich, J., et al., *Depletion and activation of microglia impact metabolic connectivity of the mouse brain.* J Neuroinflammation, 2023. **20**(1): p. 47.

39. Bartos, L., et al., *NIMG-51. 18KDA TRANSLOCATOR PROTEIN (TSPO) DECLINES IN TUMOR AND IMMUNE CELLS DURING PROGRESSION OF EXPERIMENTAL GLIOBLASTOMA.* Neuro-Oncology, 2022. **24**(Supplement_7): p. vii175-vii175.
40. Bartos, L.M., et al., *Remote Neuroinflammation in Newly Diagnosed Glioblastoma Correlates with Unfavorable Clinical Outcome.* medRxiv, 2024: p. 2024.04.23.24305825.
41. Bartos, L.M., et al., *Astroglial glucose uptake determines brain FDG-PET alterations and metabolic connectivity during healthy aging in mice.* Neuroimage, 2024. **300**: p. 120860.
42. Dinkel, L., et al., *Myeloid cell-specific loss of NPC1 in mice recapitulates microgliosis and neurodegeneration in patients with Niemann-Pick type C disease.* Sci Transl Med, 2024. **16**(776): p. eadl4616.
43. Slemann, L., et al., *Neuronal and oligodendroglial, but not astroglial, tau translates to in vivo tau PET signals in individuals with primary tauopathies.* Acta Neuropathol, 2024. **148**(1): p. 70.
44. Zatcepin, A., et al., *Regional desynchronization of microglial activity is associated with cognitive decline in Alzheimer's disease.* Mol Neurodegener, 2024. **19**(1): p. 64.
45. Gao, T., et al., *O4-09-02: REGULATION OF PRO-INFLAMMATORY AND DISEASE-ASSOCIATED MICROGLIAL ACTIVATION BY BIN1.* Alzheimer's & Dementia, 2019. **15**(7S_Part_24): p. P1256-P1256.
46. Rauchmann, B.S., et al., *Microglial Activation and Connectivity in Alzheimer Disease and Aging.* Ann Neurol, 2022. **92**(5): p. 768-781.
47. Bernier, L.P., et al., *Microglial metabolic flexibility supports immune surveillance of the brain parenchyma.* Nat Commun, 2020. **11**(1): p. 1559.
48. Orihuela, R., C.A. McPherson, and G.J. Harry, *Microglial M1/M2 polarization and metabolic states.* Br J Pharmacol, 2016. **173**(4): p. 649-65.
49. Broadwell, R.D. and A.M. Cataldo, *The neuronal endoplasmic reticulum: its cytochemistry and contribution to the endomembrane system. I. Cell bodies and dendrites.* J Histochem Cytochem, 1983. **31**(9): p. 1077-88.
50. Chen, J., et al., *Glucose-6-phosphatase-α participates in dopaminergic differentiation.* Neurol Res, 2017. **39**(10): p. 869-876.
51. Cossu, V., et al., *Obligatory role of endoplasmic reticulum in brain FDG uptake.* Eur J Nucl Med Mol Imaging, 2019. **46**(5): p. 1184-1196.
52. Müller, M.S., M. Fouyssac, and C.W. Taylor, *Effective Glucose Uptake by Human Astrocytes Requires Its Sequestration in the Endoplasmic Reticulum by Glucose-6-Phosphatase-β.* Curr Biol, 2018. **28**(21): p. 3481-3486.e4.
53. Arcus, V.L., et al., *On the Temperature Dependence of Enzyme-Catalyzed Rates.* Biochemistry, 2016. **55**(12): p. 1681-8.
54. Ababei, L. and M. Moisiu, *On the activity of glucose-6-phosphate phosphohydrolase in the red blood cells.* Blut, 1970. **20**(6): p. 363-9.
55. Welch, A., et al., *Mapping changes in mouse brain metabolism with PET/CT.* J Nucl Med, 2013. **54**(11): p. 1946-53.
56. Camandola, S. and M.P. Mattson, *Brain metabolism in health, aging, and neurodegeneration.* Embo j, 2017. **36**(11): p. 1474-1492.
57. Harris, J.J., R. Jolivet, and D. Attwell, *Synaptic energy use and supply.* Neuron, 2012. **75**(5): p. 762-77.
58. Duraj, T., et al., *Metabolic therapy and bioenergetic analysis: The missing piece of the puzzle.* Mol Metab, 2021. **54**: p. 101389.

59. Westi, E.W., J.V. Andersen, and B.I. Aldana, *Using stable isotope tracing to unravel the metabolic components of neurodegeneration: Focus on neuron-glia metabolic interactions.* Neurobiol Dis, 2023. **182**: p. 106145.
60. Varma, V.R., et al., *Brain and blood metabolite signatures of pathology and progression in Alzheimer disease: A targeted metabolomics study.* PLoS Med, 2018. **15**(1): p. e1002482.
61. Divakaruni, A.S., et al., *Analysis and interpretation of microplate-based oxygen consumption and pH data.* Methods Enzymol, 2014. **547**: p. 309-54.
62. Yépez, V.A., et al., *OCR-Stats: Robust estimation and statistical testing of mitochondrial respiration activities using Seahorse XF Analyzer.* PLoS One, 2018. **13**(7): p. e0199938.
63. Tsukioka, M., et al., *Expression of glucose transporters in epithelial ovarian carcinoma: correlation with clinical characteristics and tumor angiogenesis.* Oncol Rep, 2007. **18**(2): p. 361-7.
64. Wong, M.L. and J.F. Medrano, *Real-time PCR for mRNA quantitation.* Biotechniques, 2005. **39**(1): p. 75-85.
65. Peng, X., et al., *Molecular Characterization and Clinical Relevance of Metabolic Expression Subtypes in Human Cancers.* Cell Rep, 2018. **23**(1): p. 255-269.e4.
66. Breijyeh, Z. and R. Karaman, *Comprehensive Review on Alzheimer's Disease: Causes and Treatment.* Molecules, 2020. **25**(24).
67. Blennow, K., M.J. de Leon, and H. Zetterberg, *Alzheimer's disease.* Lancet, 2006. **368**(9533): p. 387-403.
68. Gu, X., et al., *Measurement of mitochondrial respiration in adherent cells by Seahorse XF96 Cell Mito Stress Test.* STAR Protoc, 2021. **2**(1): p. 100245.
69. Sokoloff, L., *Sites and mechanisms of function-related changes in energy metabolism in the nervous system.* Dev Neurosci, 1993. **15**(3-5): p. 194-206.
70. Sokoloff, L., *Energetics of functional activation in neural tissues.* Neurochem Res, 1999. **24**(2): p. 321-9.
71. Gargiulo, S., et al., *Mice anesthesia, analgesia, and care, Part I: anesthetic considerations in preclinical research.* Ilar j, 2012. **53**(1): p. E55-69.
72. Minoshima, S., et al., *(18)F-FDG PET Imaging in Neurodegenerative Dementing Disorders: Insights into Subtype Classification, Emerging Disease Categories, and Mixed Dementia with Copathologies.* J Nucl Med, 2022. **63**(Suppl 1): p. 2s-12s.
73. Hülsmeyer, V.I., et al., *International Veterinary Epilepsy Task Force's current understanding of idiopathic epilepsy of genetic or suspected genetic origin in purebred dogs.* BMC Vet Res, 2015. **11**: p. 175.
74. Berendt, M., et al., *International veterinary epilepsy task force consensus report on epilepsy definition, classification and terminology in companion animals.* BMC Vet Res, 2015. **11**: p. 182.
75. Kwan, P., et al., *Definition of drug resistant epilepsy: Consensus proposal by the ad hoc Task Force of the ILAE Commission on Therapeutic Strategies.* Epilepsia, 2010. **51**(6): p. 1069-1077.
76. Lane, S.B. and S.E. Bunch, *Medical Management of Recurrent Seizures in Dogs and Cats.* Journal of Veterinary Internal Medicine, 1990. **4**(1): p. 26-39.
77. Hasegawa, D., *Diagnostic techniques to detect the epileptogenic zone: Pathophysiological and presurgical analysis of epilepsy in dogs and cats.* Vet J, 2016. **215**: p. 64-75.
78. Foss, K.D. and A.C. Billhymer, *Magnetic resonance imaging in canine idiopathic epilepsy: a mini-review.* Front Vet Sci, 2024. **11**: p. 1427403.

79. Hillner, B.E., et al., *Impact of positron emission tomography/computed tomography and positron emission tomography (PET) alone on expected management of patients with cancer: initial results from the National Oncologic PET Registry.* J Clin Oncol, 2008. **26**(13): p. 2155-61.
80. Mankoff, D.A., et al., *Tumor-specific positron emission tomography imaging in patients: [18F] fluorodeoxyglucose and beyond.* Clin Cancer Res, 2007. **13**(12): p. 3460-9.
81. Belotta, A.F., et al., *Comparison of sedation and general anesthesia protocols for (18)F-FDG-PET/CT studies in dogs and cats: Musculoskeletal uptake and radiation dose to workers.* Vet Radiol Ultrasound, 2025. **66**(1): p. e13439.

7. Zusammenfassung

Die Erforschung der komplexen pathologischen Mechanismen, welche den Glukosestoffwechsel von Mikroglia im Zusammenhang mit neurodegenerativen Erkrankungen beeinflussen, erfordert die präzise Erfassung der Gegebenheiten im regulären Hirnmilieu.

Ziel dieser Arbeit war es daher, durch den neu etablierten Workflow des scRadiotracing, die Aussagekraft reiner *in vitro* Messungen des Glukosestoffwechsels durch einen unmittelbaren Vergleich mit dem *in vivo* Milieu zu evaluieren. Auf diese Weise wurde demonstriert, dass Ergebnisse aus alleinigen *in vitro* Versuchen zur Erforschung des mikroglialen Metabolismus nicht die tatsächliche komplexe *in vivo* Situation widerspiegeln, da sich die Zellen nicht naturgemäß verhalten können. Diese Erkenntnis wird durch die Daten einer Studie unserer Arbeitsgruppe besonders hervorgehoben, welche die enorme metabolische Aktivierung von Mikroglia in neurodegenerativen Erkrankungen zeigte [20].

scRadiotracing gewährleistet in diesem Rahmen die Erfassung des zellulären Glukosemetabolismus als Momentaufnahme *in vivo*. Damit können Zellen in ihrer natürlichen Umgebung erforscht werden und auch in pathologischen Modellen reale Veränderungen anzeigen. Außerdem kann die Aufnahme des Radiotracers pro Einzelzelle nachvollzogen werden und bietet sich somit als ergänzendes Hilfsmittel bei der Aufklärung von Tracer-Aufnahmemechanismen und ihrer zugrundeliegenden Zellbiologie an. Der bisher gängigen Bildgebung gehirnbezogener Erkrankungen fehlt diese zelluläre Auflösung. Zur Optimierung der Methodik werden weitere Studien mit Fokus auf Determinanten und Limitationen des scRadiotracing notwendig sein.

Insgesamt demonstriert diese Promotionsarbeit, unter Verwendung des neuartigen scRadiotracing, die eingeschränkte Vergleichbarkeit von *in vivo* und *in vitro* durchgeführten Untersuchungen des zerebralen Glukosestoffwechsels von Mikrogliazellen. Die einfache Kombinierbarkeit mit ergänzenden Methoden macht scRadiotracing zu einem wertvollen Hilfsmittel in der Grundlagenerforschung neurodegenerativer Erkrankungen.

8. Abstract

Assessment of relative cellular glucose uptake of microglia cells within the regular brain environment

The investigation of intricate pathological mechanisms influencing microglial glucose metabolism requires precise acquisition of conditions prevailing in the regular brain environment.

Consequently, the objective of this study was to evaluate the reliability of sole *in vitro* measurements of glucose metabolism by direct comparison to *in vivo* on the same cells, using the novel workflow of scRadiotracing. This approach demonstrated that results from sole *in vitro* methods for the investigation of microglial metabolism do not accurately reflect the complex *in vivo* situation, due to the cells not being able to act physiologically. This finding is highlighted by data of our previous study, indicating the tremendous metabolic activation of microglia in neurodegenerative diseases [20].

In this context, scRadiotracing allows quantification of cellular glucose uptake as snapshot *in vivo*. Hence, cells can be studied in their natural environment and may display actual alterations in disease models. Moreover, it facilitates uptake measurements of radiotracers per single cell and can be used as complementary tool for elucidating the mechanisms of radiotracer uptake and their underlying cellular biology. This cellular resolution is hitherto lacking in the neuroimaging of brain disorders. In terms of optimization, further studies are required to disclose determinants and limitations of scRadiotracing.

Taken together, this dissertation demonstrates the limited comparability of *in vivo* and *in vitro* investigations of cerebral metabolism of microglia, employing the novel scRadiotracing methodology. The straightforward integration with complementary assays emphasizes scRadiotracing as valuable tool in preclinical research of neurodegenerative diseases.

Danksagung

An erster Stelle möchte ich mich bei Herrn Prof. Dr. Dr. Matthias Brendel für die exzellente Betreuung dieser Promotionsarbeit bedanken. Er schaffte es, mich mit seiner eigenen Leidenschaft für die Grundlagenforschung stets zu motivieren und stand mir jederzeit für Fragen und Besprechungen zur Seite. Mit der Beteiligung an vielen interessanten Projekten und Fortbildungen konnte er auch bei mir die Begeisterung für Forschung wecken und mir so viele weitere Chancen ermöglichen. Sein besonderer persönlicher Umgang mit Doktoranden und Kollegen wird mir immer ein Vorbild sein.

Auch danke ich meinem Doktorvater Herrn Prof. Dr. Eckhard Wolf für die Ermöglichung der Promotionsarbeit und stets freundliche und hilfsbereite Beantwortung aller Fragen.

Meinen Doktoranden Kollegen Philipp Beumers und insbesondere Laura Bartos möchte ich herzlich für die hervorragende Zusammenarbeit und gegenseitige Unterstützung bei Projekten danken sowie die stets lockere und freundschaftliche Atmosphäre speziell auch an längeren Versuchstagen im Labor. Sie haben diese Zeit maßgeblich mitgeprägt und sie zu einem besonderen Abschnitt in meinem Leben gemacht.

Bei Rosel Oos, Giovanna Palumbo sowie Karin Wind-Mark möchte ich mich für die ausgezeichnete Einarbeitung und Unterstützung bei der Planung und Durchführung von Versuchstagen bedanken.

Mein besonderer Dank gilt überdies meinen Eltern und meiner Schwester, die mich stets uneingeschränkt unterstützt und beraten haben sowie Greta, die mich dabei meine eigentlichen Ziele im Auge behalten lies.